Deanship of Graduate Studies

Al-Quds University

Development of Myristate Analogues as Allosteric Inhibitors of BCR-ABL for Treatment of Chronic Myeloid Leukemia

Nidaa Odeh Shehadeh Eghreib

M.SC Thesis

Jerusalem-Palestine

1434-2013

Development of Myristate Analogues as Allosteric Inhibitors of Bcr-Abl for Treatment of Chronic Myeloid Leukemia

Prepared By:

Nidaa Odeh Shehadeh Eghreib

B. Sc. General Chemistry Bethlehem University

Supervisor:

Dr. Yousef Najajreh

Thesis submitted in partial fulfillment of the requirements for the Degree of Master of Applied & Industrial Technology, Department of Chemistry, Faculty of Science and Technology at Al-Quds University

1434/2013

Al-Quds University

Deanship of Graduate Studies

Applied and Industrial Technology

Department of Science and Technology

Thesis Approval

Development of Myristate Analogues as Allosteric Inhibitors of Bcr-Abl for Treatment of Chronic Myeloid Leukemia

Prepared By: Nidaa Odeh Shehadeh Eghreib

Registration No: 20812213

Supervisor: Dr. Yousef Najajreh

Master thesis submitted and accepted, Date:

The names and signatures of the examining committee members are as follows:

1- Head of Committee: Dr. Yousef Najajreh Signature:

2- Internal Examiner: Dr. Hatem Hejaz Signature:

3- External Examiner: Dr. Michel Hanania Signature:

Jerusalem – Palestine

1434/2013

Declaration

I certify that this thesis submitted for the degree of master, is the result of my own research, except where otherwise acknowledged, and this thesis has not been submitted for the higher degree to any other university or institution.

Signed: …….

Nida Odeh Shehadeh Eghreib

Date: ……

Acknowledgments

I would like to express my deep and sincere gratitude to my supervisor, Yousef Najajreh, Ph.D. Assoc. Prof. /Dean of Scientific Research / Al Quds University for the useful comments, remarks and advices through the learning process of this master thesis. His wide knowledge and his logical way of thinking have been of great value for me.

I thank Al Quds University for giving me the opportunity to achieve the M.Sc. degree. Special thanks to Professor Ibrahim Kayali / Coordinator of the Higher Studies Program for Applied Industrial Technology /Al Quds University for his support and encouragement throughout this work.

Furthermore, I would like to thank Dr. Jamal Mahajna and his team / Galilee Technology Center / Migal / Israel for providing our *in vitro* kinase data.

During this work I have collaborated with many colleagues for whom I have great regard, and I wish to extend my warmest thanks to all those who have helped me with my work in the Anticancer Drug Research Lab / Faculty of Pharmacy / Al Quds University.

Last but not least, I would like to thank to my husband, parents, and family for their kind co-operation and encouragement which help me in completion of this project.

The financial support of the German Research Foundation (DFG) is gratefully acknowledged.

Abstract:

Chronic myeloid leukemia (CML), a cancer originating in the bone marrow, causes excessive proliferation of myeloid cells. The genetic signature of the disease is the Philadelphia chromosome, created by a translocation between chromosomes 9 and 22 t(9;22). This translocation results in *BCR* and *ABL* genes fusing together. The chimeric gene product, BCR-ABL, is a deregulated tyrosine kinase that promotes cell proliferation and survival. The majority of inhibitors targeting BCR-ABL are kinase inhibitors directed against its ATP binding site. Imatinib, the first selective ATP-competitive targeted BCR-ABL inhibitor, is successful in treating most cases of early-phase CML. Nonetheless, some patients either do not respond, or develop resistance to the drug. To combat these problems, second-generation BCR-ABL inhibitors were developed, including Nilotinib and Dasatanib. It is noteworthy that none of these drugs is effective against T315I gatekeeper mutation. There have been efforts to develop kinase inhibitors with new modes of action. In this thesis, we highlight the development of 'non-ATP competitive allosteric kinase inhibitors' that inhibit kinase activity by binding to a site remote from the active site of the kinase. In native ABL, the N-terminus is myristoylated, this N-myrisotyl moiety (a small hydrophobic chain of 14 carbons) blocks the autophosphorylation activity of ABL as it inserts into a hydrophobic pocket in the kinase domain (Myristoyl Binding Pocket - MBP). This discovery stimulated us to develop sets of myristate analogues as allosteric inhibitors of BCR-ABL that bind selectively and in high specificity to the (MBP) of the ABL kinase, where a myristoyl tail is missing in the oncoprotein BCR-ABL product. Those analogues were synthesized, purified, characterized and screened for their activity in a cell-based auto-phosphorylation assay and their clonogenicity potential was also evaluated. Initial *in vitro* results demonstrate the usefulness of this approach and reveal the identification of myristate derivatives that inhibit BCR-ABL autophosphorylation activity of the native and mutated BCR-ABL carrying the "gatekeeper" mutation T315I. in this work we discuss the discovery of novel compounds (**MAJY-12**, **-26**, **-43** and **-72**) that display improved inhibitory potency against the auto-phosphorylation of BCR-ABL.

Table of Contents

List of Tables:

List of Figures:

List of Schemes:

List of Abbreviations:

CML	Chronic Myeloid Leukemia
ABL	Abelson tyrosine kinase
BCR	Breakpoint Cluster Region
T315I	Threonine 315 Isoleucine
MBP	Myristoyl Binding Pocket
SAR	Structure-Activity Relationships
ATP	Adenosine Tri-Phosphate
AKI	ATP Kinase Inhibitor
STAT	Signal Transducer and Activation of Transcription
STI571	Signal transduction inhibitor 571
MAPKs	Mitogen Activated Protein Kinases
PDGFR	Platelet Derived Growth Factor Receptor
JAK	Janus Activated Kinase
PI3K	Phosphoinositide 3-kinase
DCC	N,N-Dicyclohexylcarbodiimide
TEA	Triethylamine
NHS	N-hydroxysuucinimide
NaOEt	Sodium Ethanoate
NaOMe	Sodium Methanoate
CC	Column Chromatography
r.t.	Room temperature
$P(Ph)_3$ or TPP	Triphenylphosphine
DMF	Dimethylformamide

n-BuLi	n-Butyl Lithium
Na_2SO_4	Sodium Sulfate
H_2SO_4	Sulfuric Acid
DCM	Dichloromethane
Eth. Ac.	Ethyl Acetate
MeOH	Methanol
EtOH	Ethanol
$CHCl_3$	Chloroform
KI),	Potassium Iodide
THF	Tetrahydrofuran
NaOH	Sodium Hydroxide
$CDCl_3$	Chloroform-d
DMSO-d_6	Deuterated Dimethyl Sulfoxide d_6
R_f	Retardation Factor

Chapter one: Introduction

1. Introduction

1.1. Chronic myelogenous leukemia

Chronic myelogenous leukemia (CML) is a type of myeloproliferative disease that affects the bone marrow, in which excess red blood cells, granulocytes, and/or platelets are produced. [1] CML is a rare disease and accounts for about 15-20% of all leukemias. Clinically, the disease progresses through three distinct phases, referred to as chronic or stable, accelerated, and blast. CML is usually diagnosed during the early chronic phase of the disease. The chronic phase is characterized by expansion of cells of the granulocytic lineage that retain their ability to differentiate. Most patients are diagnosed at this stage as a result of an increased number of mature granulocytes in the peripheral blood, weight loss and splenomegaly. This phase lasts approximately 5 years on average and then the disease progresses to the accelerated phase and the blast crisis phase. These later phases are characterized by the accumulation of immature blasts in the bone marrow and the peripheral blood and loss of hematopoietic cell differentiation (Figure-1.1). [2, 3, 4] Disease progression is caused by the accumulation of molecular abnormalities, which lead to a progressive loss of the capacity for terminal differentiation of the leukemic clone. [5]

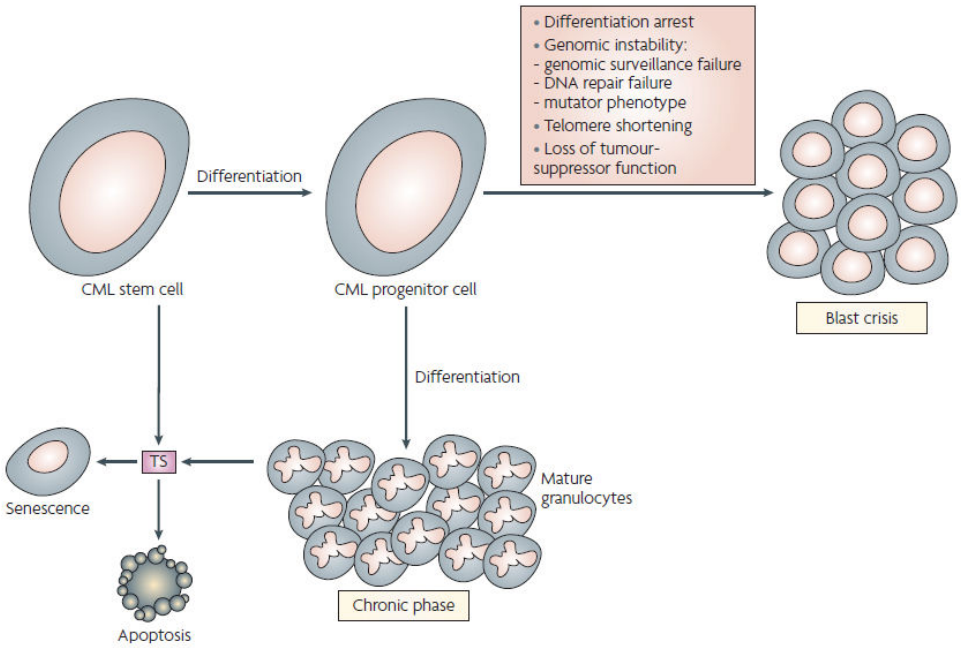

Figure-1.1: Disease progression in chronic myeloid leukemia. [3]

1.2. Philadelphia chromosome

CML disorder associated with a characteristic chromosomal translocation called the Philadelphia (Ph) chromosome, in which parts of two chromosomes, 9 and 22, swap places. This reciprocal chromosomal translocation is designated as t(9;22) in which the *ABL* ("Abelson") gene on chromosome 9 fuses to the *BCR* ("breakpoint cluster region") gene on chromosome 22. [6] The result of the reciprocal translocation is the *BCR-ABL* gene, which is located on the shorter chromosome 22. [7] The *BCR-ABL* chimeric oncogene encodes the protein p210 or sometimes p185 (p stands for "protein" and the numbers represent the molecular weight in kDa) (Figure-1.2) [8]. The presence of the Ph chromosome is the cytogenetic hallmark of CML disease.

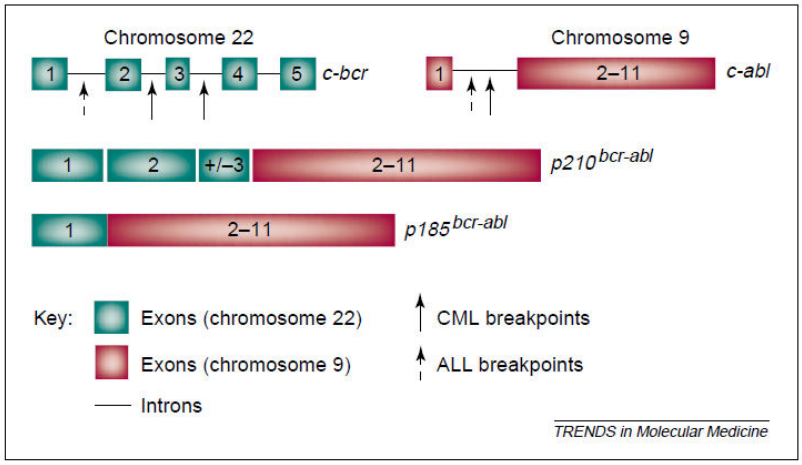

Figure-1.2: Chromosomal Translocation t(9;22) leading to BCR-ABL fusion [5]

1.3. BCR-ABL tyrosine kinase

The *ABL* proto-oncogene encodes a cytoplasmic and nuclear protein tyrosine kinase that has been implicated in processes of cell differentiation, cell division, cell adhesion, and stress response. Under normal conditions, c-ABL exists in a regulated state with very low kinase activity. Consequently, the *BCR-ABL* gene generates a fusion protein, BCR-ABL, with deregulated tyrosine kinase activity, autophosphorylates BCR-ABL and activates multiple signal transduction pathways, leading to alterations in the proliferative, adhesive, reducing growth factor-dependence, apoptosis (Figure-1.3) and abnormal interaction with extra-cellular

matrix and stroma, [9] with all of these events dependent on the tyrosine kinase activity of the BCR-ABL protein. [5, 10, 11] BCR-ABL is involved in DNA repair, causing genomic instability and potentially leading the feared blast crisis in CML. [12]

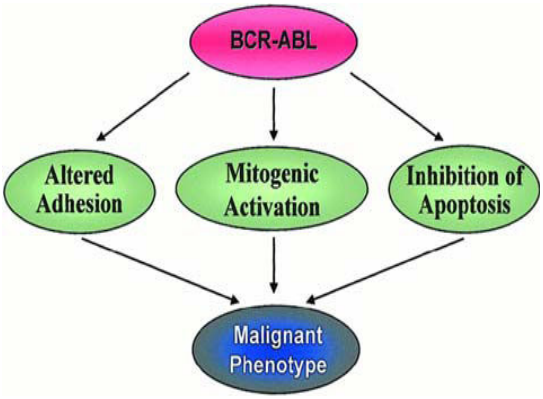

Figure-1.3: Mechanisms implicated in the pathogenesis of CML. [13]

1.4. The BCR-ABL oncogenetic pathway

ABL tyrosine kinase activity is constitutively activated by the juxtaposition of BCR so favoring dimerization or tetramerization and the subsequent autophosphorylation. This increases the number of the phosphotyrosine residues on BCR-ABL and, as a consequence, the binding sites for the SH2 domains of other proteins. [14]

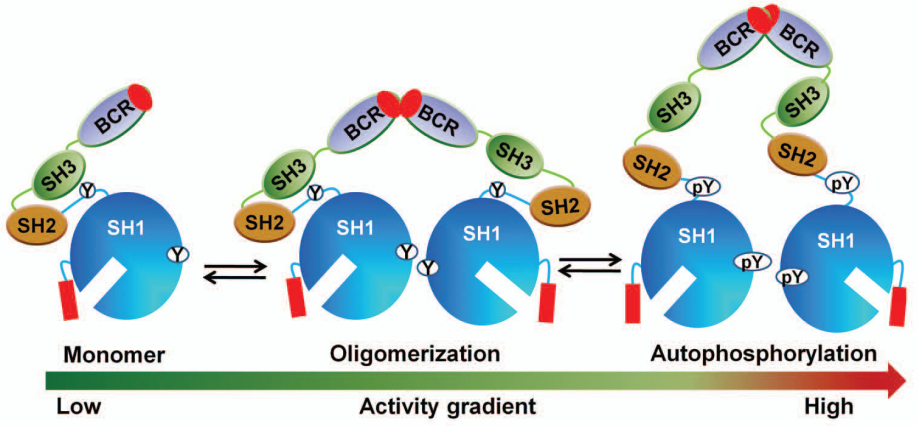

Figure-1.4: Autoregulation of BCR-ABL. Helix αI (red bar) and oligomerization domain (black) in BCR domain are shown along with SH1, SH2 and SH3 domains. Tyrosines at linker and active sites are highlighted [15].

The abnormal interactions between the BCR-ABL oncoprotein and other cytoplasmic molecules lead to the disruption of key cellular processes. Some examples could be represented by the perturbation of the Ras-MAP kinase leading to increased proliferation of the JAK-STAT (signal transducer and activation of transcription) pathway leading to impaired transcriptional activity and of the PI3K/Akt pathway resulting in increased apoptosis. All activated signaling pathways converge into a unique terminal point: loss of control of proliferation and expansion of the leukemic clone (Figure-1.5). [14]

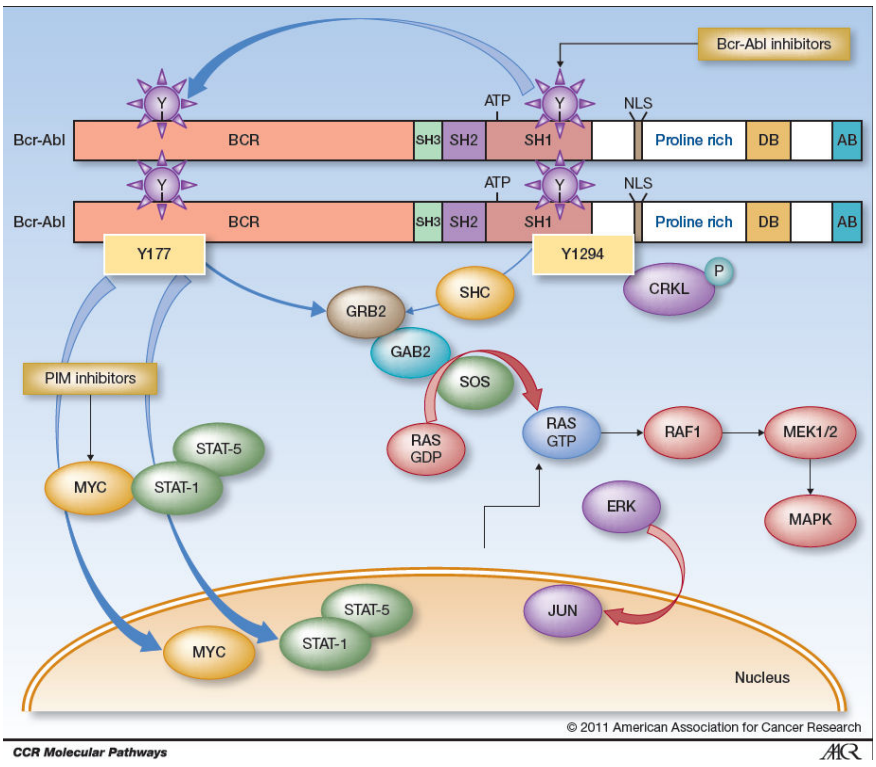

Figure-1.5: Schematic representation of the molecular pathway activated by BCR-ABL. [14]

1.5. Pharmacologic inhibitors of kinase activity

The deregulation of tyrosine phosphorylation seems to be a critical abnormality in malignant transformation, therefore the inhibition of tyrosine phosphorylation represents an attractive strategy for controlling unregulated growth and aberrant malignant behavior. However, target specificity is an important part of this strategy. High-throughput pharmaceutical technology has led to the development of families of small molecules that selectively inhibit specific

tyrosine kinases. [15] Inhibitors of kinase activity are characterized as:

(1) Type I, or "DFG-in" (ATP) competitive inhibitors, which directly compete with ATP in the ATP-binding site.
(2) Type II, or "DFG-out" ATP competitive inhibitors, which, in addition to binding the ATP binding site, also engage an adjacent hydrophobic binding site that is only accessible when the kinase is in an inactivated configuration.
(3) Non-ATP competitive inhibitors:

i) 'Allosteric inhibitors' that bind to a site remote from the active site and inhibit kinase activity. [16]

ii) Substrate competitor inhibitors such as ON012380 compound that interacts with the substrate-binding sites of these kinases. [17]

1.6. Imatinib mesylate - First generation BCR ABL kinase inhibitor

The majority of inhibitors targeting BCR-ABL are kinase inhibitors directed against its ATP binding site. [18] Imatinib mesylate (Signal Transduction Inhibitor-STI571; Gleevec), a drug introduced to the clinic, that is specific for the ABL, platelet derived growth factor (PDGF) receptor and KIT tyrosine kinases.[11, 19] Imatinib Inhibits the activity of BCR-ABL by binding to its ATP site and an adjacent allosteric site to effectively lock the kinase in an inactive conformation (Figure 1.6). [20] By using X-ray crystallography, it was found that Imatinib binds to a catalytically inactive conformation of the ABL kinase domain, often referred to as the 'DFG-out' conformation, [17] in which the highly conserved Asp–Phe–Gly (DFG) triad is flipped out of its usual position in active kinase conformations, [21] partially occluding its ATP-binding site.

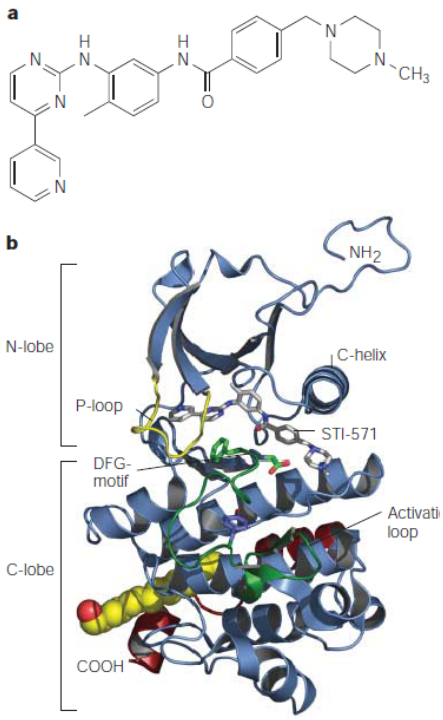

Figure 1.6: Imatinib (STI-571): an example of small-molecule inhibition of protein kinases (a) The structural formula of Imatinib. (b) Analysis of the crystal structure of the Abl kinase domain in complex with Imatinib. [22]

Imatinib binds in the cleft between the amino- and carboxy-terminal lobes of the ABL kinase domain via number of hydrophobic and hydrophilic interactions, which stabilizes the Imatinib BCR-ABL complex and prevents ATP from reaching its binding site. Thus it prevents the switch to the active conformation of BCR-ABL, thereby blocking signal transduction (Figure-1.7). [23, 24] Imatinib binds to Thr-315 (a conserved residue that is critical for recognition) located near the ATP binding pocket and controls access to the hydrophobic pocket, leading to its designation as a “gatekeeper” residue. [25, 26]

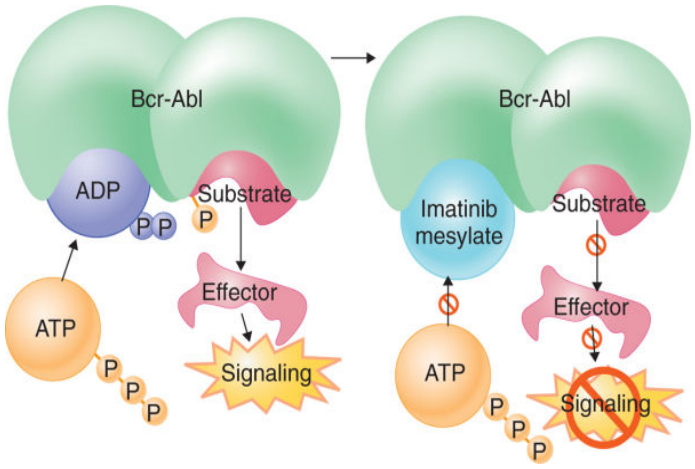

Figure-1.7: ABL kinase domain structure bound to Imatinib [24]

1.6.1. Resistance to Imatinib ("Gatekeeper" T315I mutation)

In spite of the clinical response of patients in the chronic phase CML, the majority of patients relapse upon Imatinib therapy acquiring resistance against further therapy with Imatinib. [27-29] Resistance to Imatinib is mainly related to point mutations in the BCR-ABL kinase domain which reduce the binding affinity of Imatinib to the ATP-binding domain by direct steric interference or by destabilizing the "DFG-out" conformation of the activation loop that is required for high-affinity Imatinib binding. [25] Point mutations also cause amplification of BCR-ABL and decrease cellular uptake or drug metabolism. [17] The most disturbing mutants of the BCR-ABL that induce resistance to Imatinib, is the "gatekeeper" T315I mutation (substitution of a threonine to isoleucine at position 315 of ABL) which is situated in the middle of the ATP-binding cleft. [30,31] T315I mutation eliminates the crucial hydrogen-bonding interaction required for high-affinity Imatinib-binding and the bulky isoleucine side-chain emerges into the catalytic ATP-binding pocket, sterically hindering inhibitor binding, thereby providing an explanation for its drug resistance (Figure 1.8). [32]

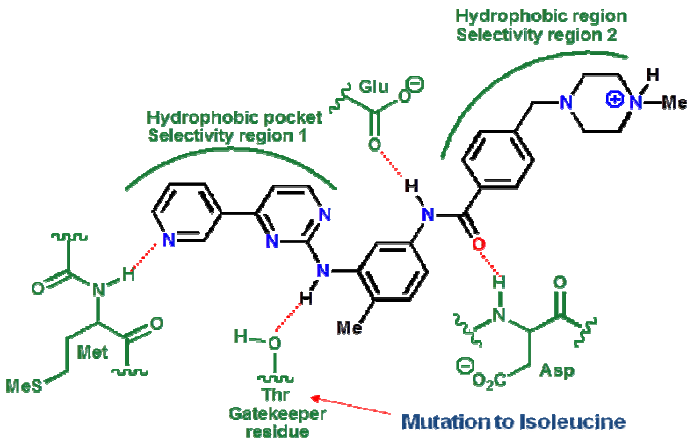

Figure-1.8: Imatinib resistance. Mutation of the gatekeeper residue to isoleucine introduces resistance (T315I mutation). [11]

1.7. Second Generation ATP-Competitive BCR-ABL Inhibitors

The emergence of resistance to Imatinib through BCR-ABL-dependent mechanisms such as kinase domain mutations, spurred the development of the second generation tyrosine kinase inhibitors (TKIs); [33] Nilotinib, Dasatinib and Bosutinib (Table-1.1). [9]

Table 1.1: List of first and second generation of BCR-ABL tyrosine kinase inhibitors

Compound	Description	Structure
First generation BCR ABL kinase inhibitors		
Imatinib	BCR-ABL	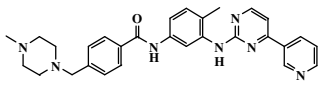
Second generation BCR ABL kinase inhibitors		
Nilotinib	BCR-ABL	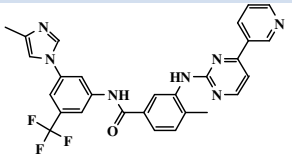
Dasatinib	BCR-ABL	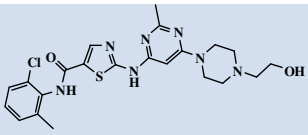
Bosutinib	BCR-ABL	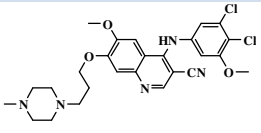

Nilotinib, like Imatinib, recognizes and binds the inactive "DFG- out" conformation of the ABL kinase. [34, 35] Dasatinib inhibits both the active and inactive conformations of the kinase domain and has a much broader specificity profile, with activity against SRC kinases, c-KIT, PDGFR, ABL and many others. [33] Dasatinib overcomes most Imatinib resistant mutations with the exception of T315I. [36] Although both compounds inhibit most of the mutations that induce resistance to Imatinib, neither compound is capable of inhibiting the "gatekeeper" T315I mutation. Both Dasatinib and Nilotinib make a hydrogen bonding interaction to the side-chain hydroxyl group of T315I, and their binding modes are incompatible with introduction of a large isobutyl side chain of isoleucine. [37, 38] Bosutinib has dual SRC/ABL tyrosine kinase inhibitory activity, but no significant activity against c-KIT and PDGFR. This compound also decreases the phosphorylation of many downstream cellular proteins including MAPKs, STAT5 and others and inhibits proliferation of CML cells. Bosutinib showed *in vitro* activity against all Imatinib resistant mutants except T315I. [17]

The T315I mutation is the most resistant to inhibition because of a combination of several factors, including steric hindrance of drug binding, loss of a key hydrogen-bonding interaction with the T315 side chain hydroxyl group exploited by Imatinib, Nilotinib and Dasatinib and potentially through increasing aberrant intrinsic kinase activity accompanied by aberrant substrate phosphorylation. [39]

1.8. Other BCR-ABL tyrosine kinase inhibitors

The clinical importance of the gatekeeper mutation T315I led to synthesis of novel inhibitors that are able to circumvent this mutation. [40] Several compounds targeting T315I are being developed, which are more potent and/or are active against the emerging Gleevec resistant BCR-ABL clones in treated patients and may overcome resistance. Some of these inhibitors with their structures and description are shown in table 1.2-a & b.

Table 1.2-a: List of BCR-ABL tyrosine kinase inhibitors

Compound	Description	Structure
AP23464	A dual SRC/ABL inhibitors and exhibits only moderate potency toward T315I BCR-ABL.	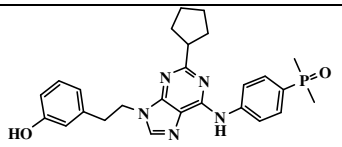
PD180970	Inhibits Bcr/Abl tyrosine phosphorylation at an IC50 of 170 nM It also has activity against Imatinib mesylate–resistant K562 cells and Ba/F3-P210 cells expressing BCR/ABL kinase domain mutations found in patients with CML resistant to imatinib mesylate. [41]	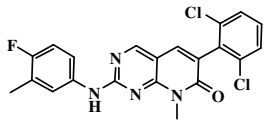
HG-7-85-01	- A 'hybrid design' between Dasatinib and the Nilotinib, and is capable of inhibiting T315I BCR- ABL - It has the ability to potently inhibit kinases that possess either a threonine or a larger hydrophobic residue, such as isoleucine, methionine, or phenylalanine. [42]	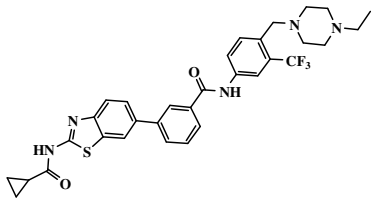
AP24163	Dual SRC/ABL inhibitors and exhibits only moderate potency toward T315I BCR-ABL. AP24163 inhibits the gatekeeper mutant of BCR-ABL by employing both mechanisms by disrupting the hydrophobic spine and by constraining the flexibility of P-loop. [43]	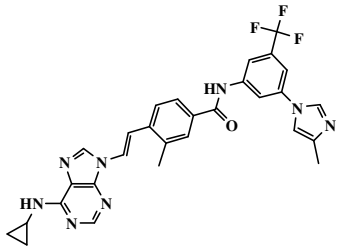
Compound 14	A 'hybrid design' between PD166326 and Imatinib, disrupts the assembly of the hydrophobic spine, thereby locking the kinase in an inactive 'DFG-out' conformation. [44]	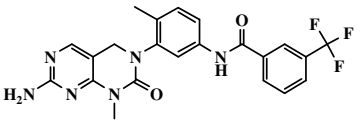

Table 1.2-b: List of BCR-ABL tyrosine kinase inhibitors

Compound	Description	Structure
Ponatinib	ABL/SRC inhibitor which has demonstrated activity against all tested mutants that are resistant to Imatinib, including T315I. [45]	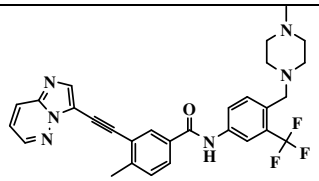
PD166326	It has the ability to bind the BCR/ABL kinase domain in either the active or inactive conformation. PD166326, have activity against many of the most prevalent Imatinib resistant except for P210 T315I. [46]	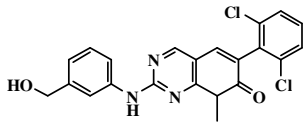
SGX393	A potent inhibitor of native and T315I-mutant BCR-ABL kinase. SGX393 suppresses outgrowth of all BCR-ABL escape mutants when combined with Nilotinib or Dasatinib.[47]	Not published yet
PHA-739358	A pan–Aurora kinase inhibitor with activity against T315 BCR-ABL kinase. PHA-739358 binds to the active conformation of the mutant kinase in a mode that accommodates the substitution of isoleucine for threonine, thus avoiding steric clash. [9]	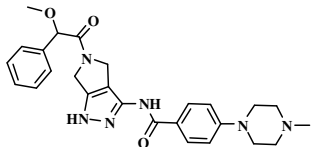
Compound 4	One of the series of the alkyne containing type II inhibitors that can circumvent the T315I BCR-ABL "gatekeeper" mutation by bridging the ATP and allosteric binding site using a linker segment that can accommodate a larger gatekeeper residue. [48]	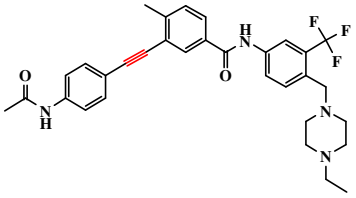
DCC-2036	- The binding, DCC-2036 to ABL or ABL/T315I induces and stabilizes the "DFG-out", catalytically inactive conformation of the kinase domain, precluding phosphorylation of activation loop residue Y393 and a critical event preceding full catalytic activation of ABL kinase. [49]	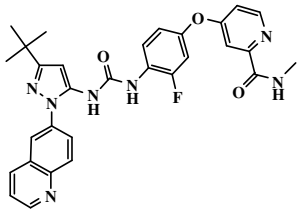

1.9 Non-ATP-competitive inhibitors of BCR-ABL

A potential alternative approach to ATP-competitive BCR-ABL inhibition is to use molecules that inhibit the kinase activity by non-ATP competitive inhibitors which are divided into two types: 1) Allosteric mechanism. 2) Substrate competitor inhibitors. This strategy has the advantage that the Imatinib-resistant mutants are unlikely to be resistant to such inhibitors, owing to the different binding sites. In addition non-ATP competitive kinase inhibitors can be highly selective for a particular kinase because they can exploit non-conserved kinase regulatory mechanisms.

Myristoyl binding pocket (MBP) was reported few years ago as an allosteric site and a potential drug target. [50] ABL tyrosine kinase has an N-terminal ‘‘Cap’’ that is implicated in regulating the autophosphorylation activity of the ABL kinase. [51] The N-terminus of c-ABL is myristoylated, this N-myrisotyl moiety blocks the activity of ABL as it binds to a hydrophobic pocket (Myristoyl Binding Pocket - MBP) located in the C lobe of the c-ABL kinase domain (Figure 1.9). [52]

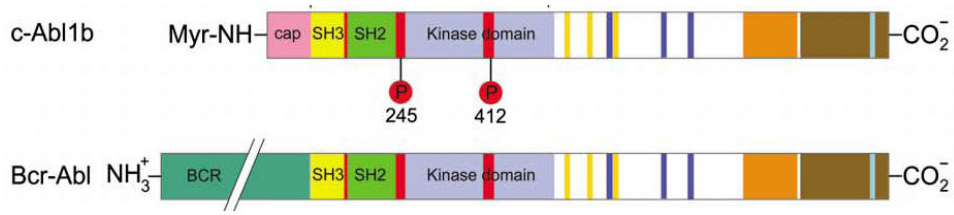

Figure-1.9: Schematic diagram showing the domain structures of c-ABL1b, and BCR-ABL [52].

When the N-terminus myristate binds to the hydrophobic pocket it induces a conformational changes that enable intra-molecular docking of the SH2 domain to the kinase domain through an interlocking network of hydrogen bonding interactions [50] thereby enforcing an auto-inhibited conformation, a process termed “Capping”. This internal docking requires the induction of a sharp bend in the C-terminal helix at the base of the kinase domain. [37] Therefore the lack of the amino-terminal auto-inhibitory region of ABL in the BCR-ABL fusion protein might play a role in the activation of BCR-ABL (Figure-1.10). [52] In the context of the t(9;22), the N-terminal auto-inhibitory “Cap” region is substituted by the BCR portion

of the fusion protein. The absence of the "Cap" region allows the BCR-ABL to "escape" auto-inhibition contributing to the constitutive activation of its kinase activity. [49]

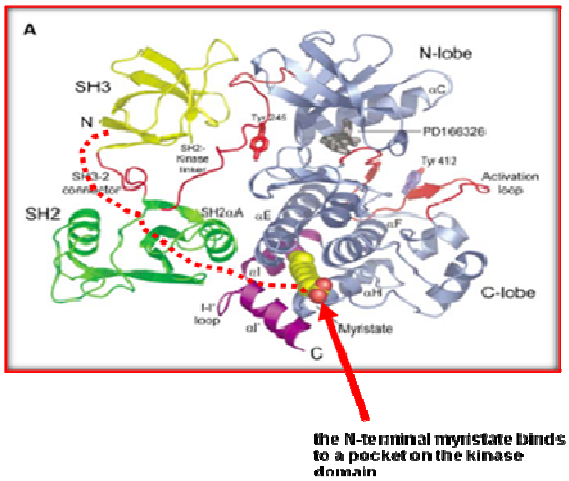

Figure-1.10: The inhibition of the ABL-kinase activity by "capping" [52]

Interestingly, small molecules that mimic the interaction of the cap myristoyl group with the C-lobe are also effective c-ABL kinase inhibitors, suggesting that the myristic-acid-binding pocket is a unique feature that allosterically controls the kinase active site. [52] High throughput screening for inhibitors of BCR-ABL dependent cell proliferation resulted in the identification of a lead compound that was subsequently modified to give (GNF-2) [50] as a selective non-ATP competitive inhibitor of cellular BCR-ABL kinase activity that targets the myristate binding site. [53] A co-crystal structure showed that binding of GNF-2 to the myristate pocket induces a bent conformational of αI helix that stabilizes the autoinhibited form of ABL. The conformations of the myristate and GNF-2 complexes are comparable to each other. In addition, GNF-2 was shown to inhibit the kinase activity of non-myristoylated c-ABL more potently than that of myristoylated c-ABL by binding to the myristate-binding pocket in the C-lobe of the kinase domain. [54] As expected, most of the interactions between GNF-2 and the protein are hydrophobic. [55]

Mutations of three residues near the mouth of the myristate-binding site (C464Y, P465S and E505K) were reported to cause complete resistance to the binding of GNF-2, presumably for steric reasons (Figure-1.11, Table 1.3). [55] GNF-2 could inhibit the phosphorylation of Bcr–

ABL and STAT5 in all mutants except the three mentioned myristate-site mutations and the 'gatekeeper' T315I mutation. The myristate-site mutations directly interfere with drug binding, whereas the non-myristate-site mutants function through a different mechanism, which may involve disfavoring the inhibited conformation induced after binding of GNF-2.

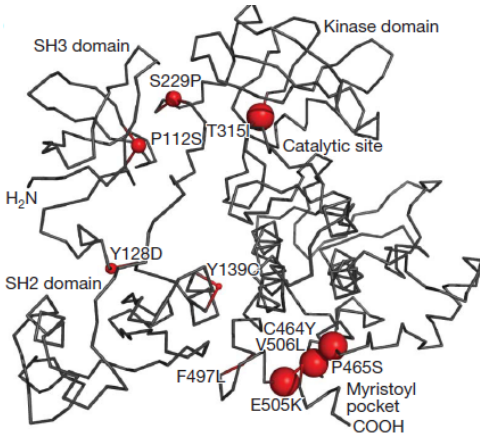

Figure-1.11: Location of BCR–ABL GNF-2 resistance mutations. Mutations indicated by red spheres on ABL with size proportional to the degree of resistance. [56]

Table-1.3: IC_{50} for growth inhibition by Imatinib or GNF-2 for wild-type and mutant BCR–ABL transformed Ba/F3 cells. The numbers of colonies that emerged after 12 days in the presence of 20 µM GNF-2 are indicated. [56]

Mutation	**IC_{50} (µM)**		**No. of Resistant colonies**
	Imatinib	**GNF-2**	
Bcr–ABL	0.48	0.26	0
T315I	10.0	10.0	24
P112S	0.64	5.28	13
Y128D	0.40	4.07	19
Y139C	0.41	2.22	14
S229P	0.85	6.06	19
C464Y	0.30	10.0	24
P465S	0.24	10.0	24
F497L	0.13	1.93	1
E505K	0.24	10.0	24
V506L	0.23	1.25	11

A recent study showed that Dasatinib is capable of cooperating with GNF-2 in inhibiting the proliferation of Ba/F3 cells carrying the native or the T315I mutated BCR-ABL, whereas no cooperation was observed between GNF-2 and (Imatinib and Nilotinib) in controlling the proliferation and colonogenicity of the parental Ba/F3 cells. Indeed, the cooperation with Dasatinib was more potent than the one observed with Imatinib or Nilotinib. Presence of 1 μM of the ABL kinase inhibitors reduced the IC_{50} of GNF-2 from 25 μM to 10.5 μM, 13 μM, and 3.5 μM when Imatinib, Nilotinib and Dasatinib were used, respectively (Table-1.4). [56] The enhanced activity of the combination of GNF-2 with Dasatinib might be due to the inhibitory activity of Dasatinib on SRC kinase which is involved in STAT5α phosphorylation, [56] in addition that GNF-2 introduces changes in the overall conformations of BCR/ABL-T315I, which renders the ATP-binding site more accessible to Dasatinib. [49]

Table-1.4: Cooperation between GNF-2 and AKIs in colonogenicity inhibition of Ba/F3 p185 BCR-ABL T315I cells. [56]

	AKIs	**IC_{50}(μM)**
GNF-2		25 ± 0.707
GNF-2	Imatinib (0.1μM)	14.8 ± 3.535
GNF-2	Nilotinib (0.1μM)	16.5 ± 1.606
GNF-2	Dasatinib (0.1μM)	13 ± 1.414
GNF-2	Imatinib (1μM)	10.5 ± 0.707
GNF-2	Nilotinib (1μM)	13 ± 3.535
GNF-2	Dasatinib (1μM)	3.3 ± 0.354

GNF-2 presents an intriguing lead molecule for the design of allosteric inhibitors of BCR-ABL, which could conceivably inhibit the activity of Imatinib-resistant BCR-ABL kinase-domain mutants. [50] GNF-5, an analogue of GNF-2 possessing similar cellular BCR–ABL inhibitory activity but having more favorable pharmacokinetic properties, [55] is capable of synergizing with ATP-competitive inhibitors such as Nilotinib to inhibit the proliferation of T315I BCR-ABL (Figure 1.12). One possible explanation for the cooperative effect of GNF-5 and Nilotinib is that GNF-5 binding to the myristate pocket can cause dynamic perturbations to residues in the ATP-binding site (conformational changes) and provides a mechanism by which synergistic interactions between these two sites could occur and stabilizes the inactive form of the T315I mutant. [55]

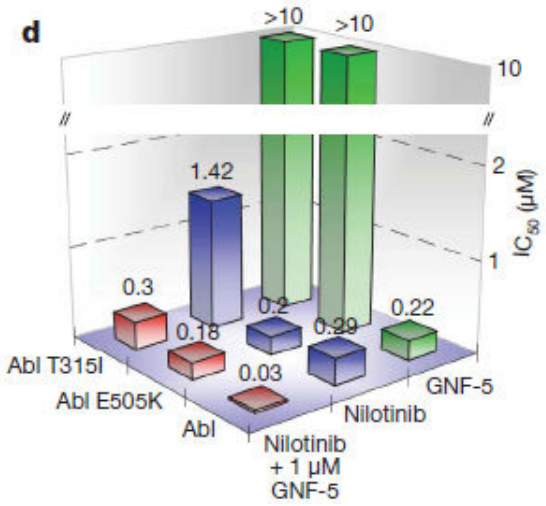

Figure-1.12: Cellular and enzymatic inhibition of wild-type and mutants by combination treatments. IC_{50} for inhibition of wild-type, E505K and T315I ABL kinase activity by GNF-5, Nilotinib or a combination of the two at an ATP concentration of 20 µM. [55]

More novel compounds have been developed that can effectively target the BCR-ABL myristate binding site, but as expected, all the compounds are inactive on T315I mutant and the myristate-binding-site mutant E505K. Some of these analogues with 5- to 10-fold improved against wild-type and some BCR-ABL mutants such as E255K relative to GNF-2 (Table-1.5). [53]

Table-1.5: BCR-ABL Structure–Activity Relationships for 4,6-Disubstituted Pyrimidines [53]

Structure	Compound code	Ba/F3[a]	BCR-ABL[b]
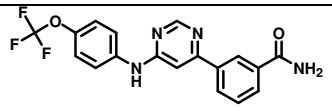	GNF-2 (**1**)	>10	0.14
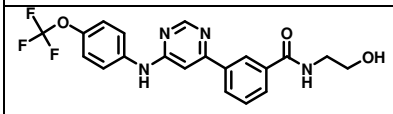	GNF-5 (**2**)	>10	0.43
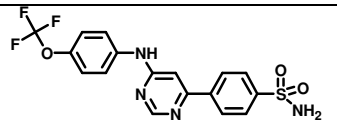	**5g**	>10	0.12
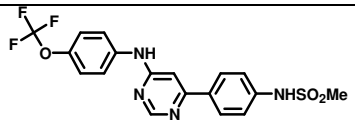	**5h**	2.21	0.04
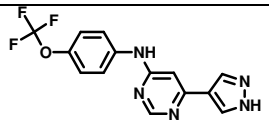	**6a**	>10	0.09
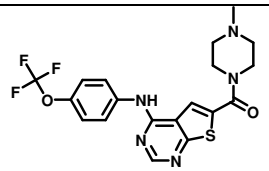	**14d**	2.69	0.048
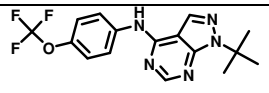	**21j**	7.3	0.16
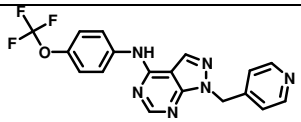	**21k**	>10	2.96
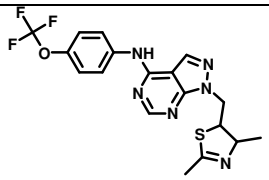	**21l**	>10	6.92

[a] Cytotoxicity (EC_{50}, μM) on parental Ba/F3. [b] Antiproliferative activity (EC_{50}, μM) on wt BCR-ABL-Ba/F3

Another regulatory site of the BCR-ABL kinase is the substrate-binding sites (Figure 1.13). ON012380 compound interacts with this site, perhaps through a covalent interaction, and exhibits low nanomolar activity against Imatinib-resistant BCR–ABL mutants, including T315I. [18] ON012380 showed a 10-fold stronger inhibition of wild-type BCR–ABL compared with Imatinib. It inhibits the growth of cells expressing the wild-type BCR–ABL protein and

all of the Imatinib-resistant kinase domain mutations, even T315I, at a concentration of less than 10 nM. ON012380 also works synergistically with Imatinib to inhibit wild-type BCR–ABL. [57]

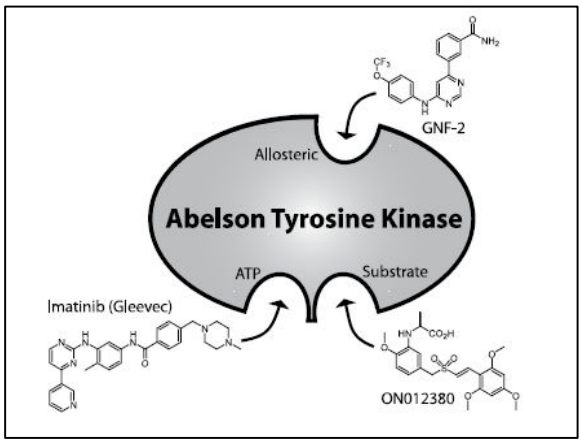

Figure-1.13: GNF-2, Imatinib and ON012380 binding to different binding sites in the kinase domain. [58]

Aim of this work:

In the current work we aim to explore the idea of targeting leukemia cancer cells with novel molecular entities that bind selectively and in high specificity to the hydrophobic pocket of the Abl kinase, where a myristoyl tail with a long hydrocarbon chain scaffold is bound in the auto-regulating process of wild type Abl, but is missing in the oncoprotein Bcr-Abl product. Since myristate being still the only known inhibitor, we have launched an investigation to explore the possibility of modifying the myristoyl scaffold in order to produce potential new binders that could exploit interactions with side chains and main chain of the MBP. We demonstrate the combination of modeling, synthesis and biological experiments that have led to the discovery of mainly novel inhibitors that are based on the myristoyl scaffold.

Chapter Two: Results and Discussion

2. Results and Discussion

The recently published crystal structures of c-ABL with the N-myristoyl moiety form the basis for computerized structure based drug design methods, [50] which enabled Dr. Amiram Goldblum's lab at the Hebrew University to propose sets of candidate derivatives of myristate that could provide effective inhibitors of BCR-ABL by targeting the MBP in the oncoprotein with high affinity. * Series of myristate mimics were synthesized and screened in biochemical and biological relevant assays. They are functionally evaluated for their potency to inhibit the auto-phosphorylation in Ba/F3 BCR-ABL transfected cells carrying either the native or the T315I mutated form.

2.1 Synthetic Chemistry

The synthesized compounds were divided into two main groups: I) aromatic myristate analogues and II) aromatic–amide myristate analogues (Figure-2.1). Two different synthetic methodologies were used to achieve the sketched structures.

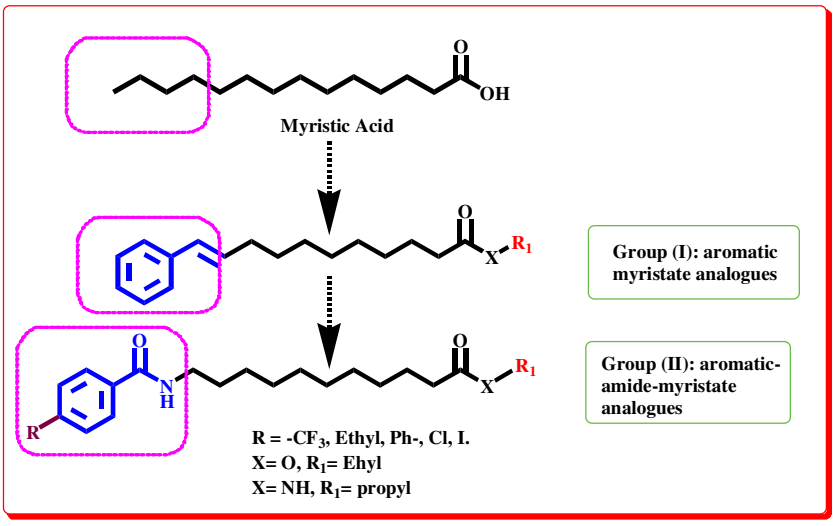

Figure-2.1: Rational for developing the aromatic-myristate analogues

*** Personal interview with Dr. Amiram Goldblum at the Hebrew University**

2.1.1 Synthesis of aromatic myristate analogues (Group (I)):

The first subgroup of compounds we started to synthesize was the aromatic containing myristate derivatives. Such subgroup could be categorized according to the position of the aromatic moiety along the carbon skeleton a) those with aromatic ring (including phenyl and naphthyl derivatives) at the ω-terminus (Figure-2.2. **A**), b) with aromatic ring inserted in between the carbon backbone (Figure-2.2. **B**) and the naphthyl derivatives (Figure-2.2. **C**).

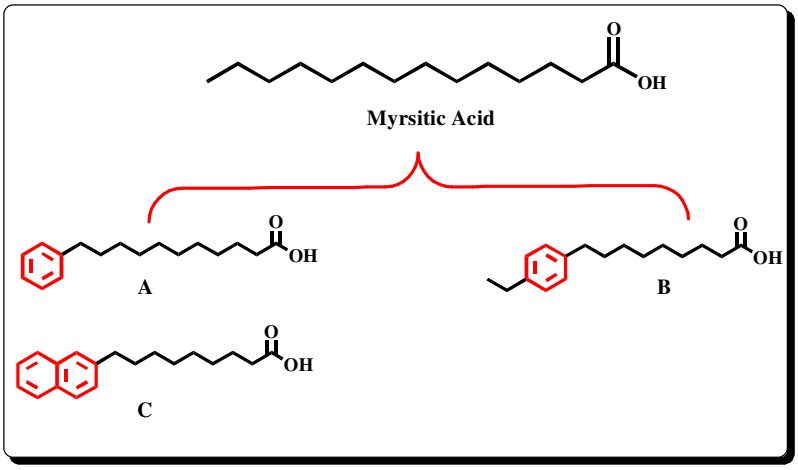

Figure-2.2: Aromatic myristate sub-categories: (**A**) aromatic ring at the ω-terminus, (**B**) aromatic ring along the backbone, (**C**) the naphthyl derivatives.

The aromatic myristate sub-categories (**A, B** and **C**) were synthesized using the Wittig olefination methodology where triphenylphosphonium ylide of the carboxy protected alkyl halide is combined with the corresponding aldehyde under strong basic conditions.

2.1.1.1 Synthesis of Subgroups A & B: Phenyl-myristate analogues

Synthesis of this group was starting with the commercially available n-bromoalkanoic acids (8-bromooctanoic **(1)** and 10-bromodecanoic **(2))** in a multistep process as shown in scheme 2.1. Reaction progress was monitored using TLC in all steps. Scheme-2.1 describes the synthesis of (9-(4-ethylphenyl)-non-8-enoic acid *Z*-(**18**), and *E*-(**19**), 9-(4-nitrophenyl)-non-8-enoic acid *Z*-(**20)** and *E*-(**21**), 11-phenylundecenoic acid **(22, 23)** via conversion of the n-bromoalkanoic acids (**1, 2**) to the corresponding ethyl esters **(4,5)** in refluxing acidic ethanol (or methanol in case of **(3)**). The n-bromoalkanoic acid ethyl esters (8-bromooctanoic acid

methyl ester **(3)**, 8-bromoctanoic acid ethyl ester **(4)**, or 10-bromodecanoic acid ethyl ester **(5)** were transformed to the triphenylphosphonium bromide salts [(9-ethoxycarbonylnonyl)-triphenylphosphonium bromide **(6)**, (7-ethoxycarbonylheptyl)-triphenylphosphonium bromide **(7)**, (7-methoxycarbonylheptyl)-triphenylphosphonium bromide **(8)**] by continuous refluxing in dry dioxane with a slight excess of triphenylphosphine (TPP). The preparation of the phosphonium intermediate was laborious and demanded very long time of refluxing in high boiling solvents.

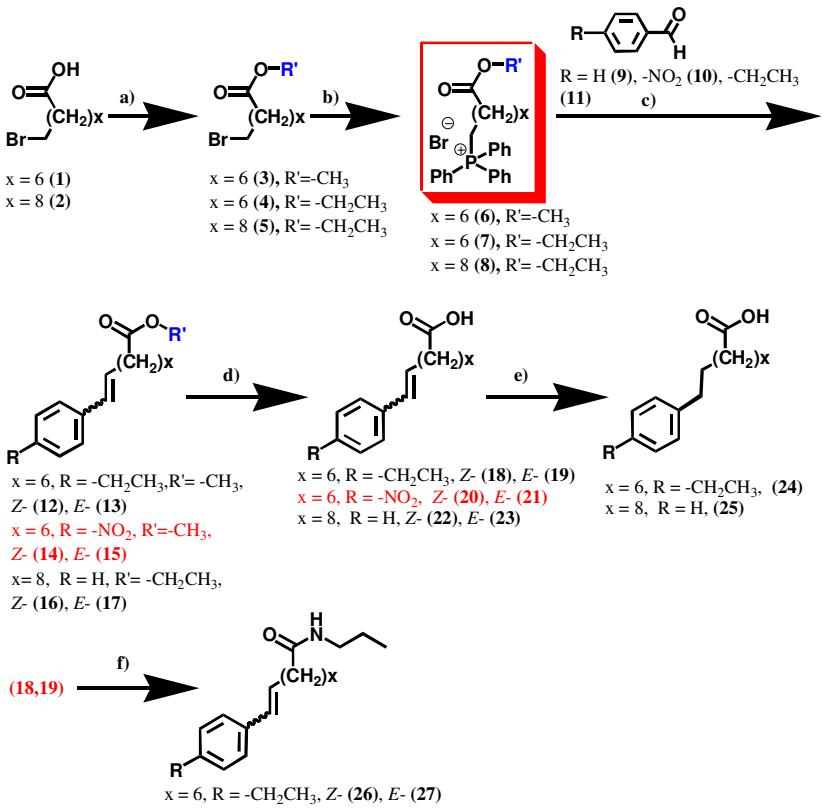

Scheme-2.1: Synthesis of the aromatic myristate analogues.

Reagents and conditions: (a) Ethanol / methanol, H^+, reflux 12 hrs, evaporation, extraction with ethyl acetate against 5%$NaHCO_3$, drying $MgSO_4$, evaporation; (b) $P(Ph)_3$, dioxane, reflux 96 hour (c) Dry THF, cooling to -78 °C under N_2, n-BuLi (1.6M) ➔ room temperature 1 hr, ➔ -78 ºC, 1.2eq aldehdyde (benzaldehyde (9), *p*-nitrobenzaldehyde (10), or ethyl benzaldehyde (11)), ➔ room temperature 3 hrs, washing with 5% $NaHCO_3$, evaporation to dryness, column chromatography; (d) 5%NaOH, MeOH-H_2O (2:1; v/v), 5 hrs at room temperature; 5% HCl, extraction (DCM/H_2O) (e) H_2(g) Pd-C, 100 psi, 4 hrs; (f) 1.1 equivalent DCC, 1.1 equivalent NHS, 2 equivalents n-propylamine.

The synthetic strategy used for preparing **(12-17)** exploited Wittig olefination methodology

where triphenylphosphonium ylide of alkanoic ester is fused with the corresponding aldehyde (benzaldehyde **(9)**, 4-nitrobenzaldehyde **(10)**, 4-ethylbenzaldehyde **(11)**) under strong basic conditions. The olefination step was tried using different conditions. First we have been trying the classical phase transfer conditions using high concentration of 50% aqueous NaOH or KOH. This afforded no detectable desired products. Later we also have tried to use different concentrations of alkoxides (NaOMe or NaOEt) as bases but this also was not successful. The organic base n-butyl lithium (n-BuLi 1.6M) was used, which gave reasonable yields of the desired products with additional by-products, which were also detected. However, the n-BuLi was not absolutely regioselective and resulted in the formation of high ratio of *E*- with little amount of the *Z*- isomers. The reaction was performed in dry THF under inert conditions and at -78 °C. After completion of the reaction (as judged by TLC) the product (9-(4-ethylphenyl)-non-8-enoic acid methyl ester (*Z*-**12**, *E*-**13**), 9-(4-nitrooxyphenyl)-non-8-enoic acid methyl ester (*Z*-**14**, *E*-**15**), 11-phenylundec-10-enoic acid ethyl ester (*Z*-**16**, *E*-**17**)) was purified using silica gel chromatography in low to modest yields (23%, 20%, 37.5%) respectively. The purification of these lipophilic compounds turned to be not easy task especially when trying to separate *Z*- and *E*-regioisomers. After hydrolysing the methyl or ethyl ester under basic conditions (5%NaOH) using and neutralization the aromatic alkenoic acid, (9-(4-ethylphenyl)-non-8-enoic acid **(18, 19)**, 9-(4-nitrooxyphenyl)-non-8-enoic acid **(20, 21**), 11-phenylundec-10-enoic acid **(22, 23)** were collected. Based on ^{1}H-NMR analysis the product **(22, 23)** was a mixture of *E*- 90% and *Z*-olefin 10%.

Since the *p*-nitrobenzaldehyde **(10)** contains no acidic protons and it is more reactive than other aldehydes, the synthesis of compound **(20, 21)** was a model reaction to help us find the conditions that could be generalized to other compounds using similar or modified procedure to improve the yield and the regioselectivity.

The aromatic acid compounds **(19)** and **(23)** were then reduced to give rise to the saturated aromatic alkanoic acids [9-(4-ethylphenyl)-nonanoic acid **(24)**, 11-phenylundecanoic acid **(25)**]. In addition, the unsaturated acids **(18,19)** were coupled to n-propylamine using standard peptide chemistry affording the amide analogues 9-(4-ethylphenyl)-non-8- enoic acid propylamide **(26,27)** respectively.

2.1.1.2 Subgroup C: 2-Naphthyl-myristate analogues

The following compounds were prepared to see whether the MBP is wide enough to accommodate such fused aromatic system. Naphthyl myristate derivatives **(28,29, 30)** were synthesized using the same methodology used in the synthesis of phenyl-myristate analogues. Naphthyl aldehyde was used to react with (7-ethoxycarbonylheptyl)-triphenylphosphonium bromide **(7)** to produce 9-naphthalen-2-yl-non-8-enoic acid ethyl ester **(28),** which was then hydrolyzed under basic condition to afford 9-naphthalen-2-yl-non-8-enoic acid **(29)**. **(28)** was also reduced to the saturated aromatic alkanoic ester 9-naphthalen-2-yl-nonanoic acid ethyl ester **(30).** (Scheme-2.2)

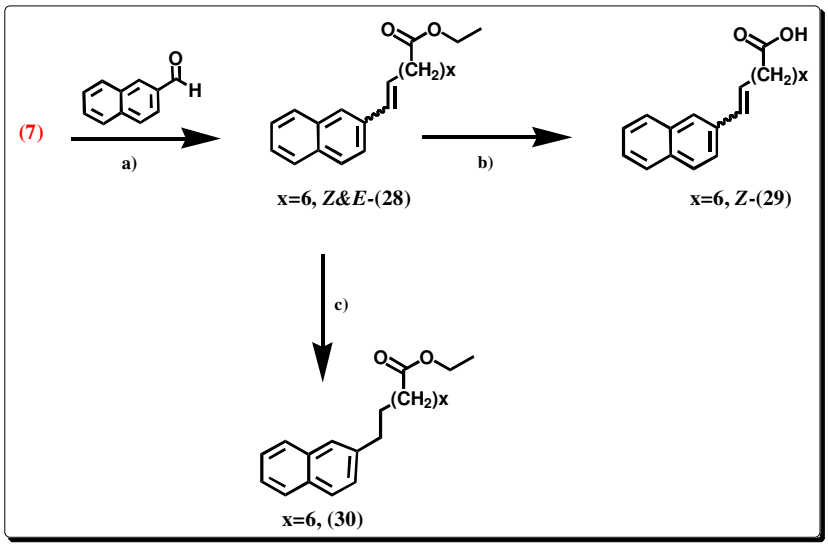

Scheme-2.2: Synthesis of naphthyl-myristate derivatives.

Reagents and conditions: (a) Dry THF, cooling to -78 °C under N_2, n-BuLi (1.6M) ➔ room temperature 1 hr, ➔ -78 ºC, 1.0eq naphthaldehyde, ➔ room temperature 3 hrs, washing with 5% $NaHCO_3$, evaporation to dryness, column chromatography; (b) 5%NaOH, MeOH-H_2O (2:1; v/v), 5 hrs at room temperature; 5% HCl, extraction (DCM/H_2O); (c) H_2(g) Pd-C, 100 psi, 4 hrs.

Based on the assumption that hydrophobic interactions are significant in the binding of myristate analogues to MBP [55], we decided to evaluate the biological activity of olefin containing intermediates ester/acids and amides **((12,13), (18,19), (28,29)** and **(26,27)** respectively.

2.1.2 Synthesis of Aromatic-Amide Myristate analogues (Group (II)):

Since the aromatic ring conjugated to double bond in group (I) have shown improved activity compared to myristic acid, we thought that replacing the alkene moiety with amide group capable of participating in hydrogen bond system, which would enhance the affinity of predicted analogues with the (MBP). To that end a series of aromatic-amidated-myristate analogues were synthesized and the biological activity was assessed against BCR-ABL positive leukemia cells.

The synthesis of this series of compounds was achieved in three steps process. The first step was the electrophilic amination of the corresponding bromoalkanoic acid [**1**, **2** and 11-bromoundecanoic acid **(31)**] using excess of aqueous ammonium hydroxide to afford the amine alkanoic acid [8-aminooctanoic acid **(32)**, 10-aminodecanoic acid **(33)**, 11-aminoundecanoic acid **(34)**] respectively (Scheme-2.3). Then the carboxyl terminal of the amine alkanoic acid was protected with ethyl (or methyl **(67))** ester in refluxed alcoholic solution under acidic conditions. The hydrochloride ammonium salt of the corresponding ethyl esters [8-aminooctanoic acid ethyl ester **(35)**, 10-aminodecanoic acid ethyl ester **(36)**, 11-aminoundecanoic acid ethyl ester **(37)**] were purified by crystallization from cold ethanol.

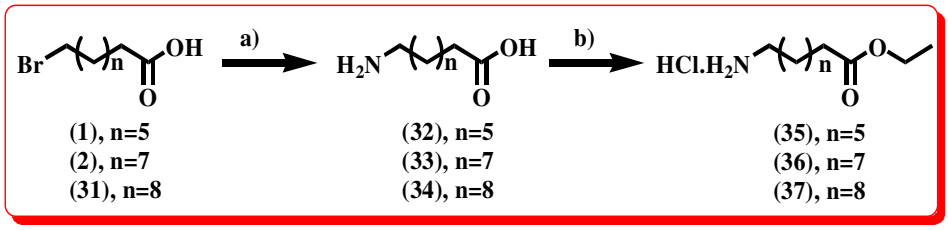

Scheme-2.3: Synthesis of amino-alkanoic acid ethyl esters.

Reagents and conditions: (a) 5 equivalents NH_4OH 25%, 30 hours at room temperature, evaporation to dryness; (b) 25ml EtOH, HCl gas at 0°C, reflux, TLC MeOH: $CHCl_3$; 5:95; v/v; I_2, evaporation to dryness.

The amino-alkanoic acid ethyl esters were then coupled to aromatic carboxylic acids **(38, 41, 43, 45, 47, 49, 52, 56, 60, 62, 66)** using DCC/NHS as a coupling agent to give rise to the

aromatic amidated myristate analogues **(39, 40, 42, 44, 46, 48, 50, 51, 53, 54, 55, 57,58,59, 61, 63,64,65, 67)** (Scheme 2.4). Compound **(44)** was also synthesized using benzoic anhydride or benzoyl chloride. The overall yields in the three steps ranged between 50% for **(44)**, 91% **(37)** and 100% **(34)**

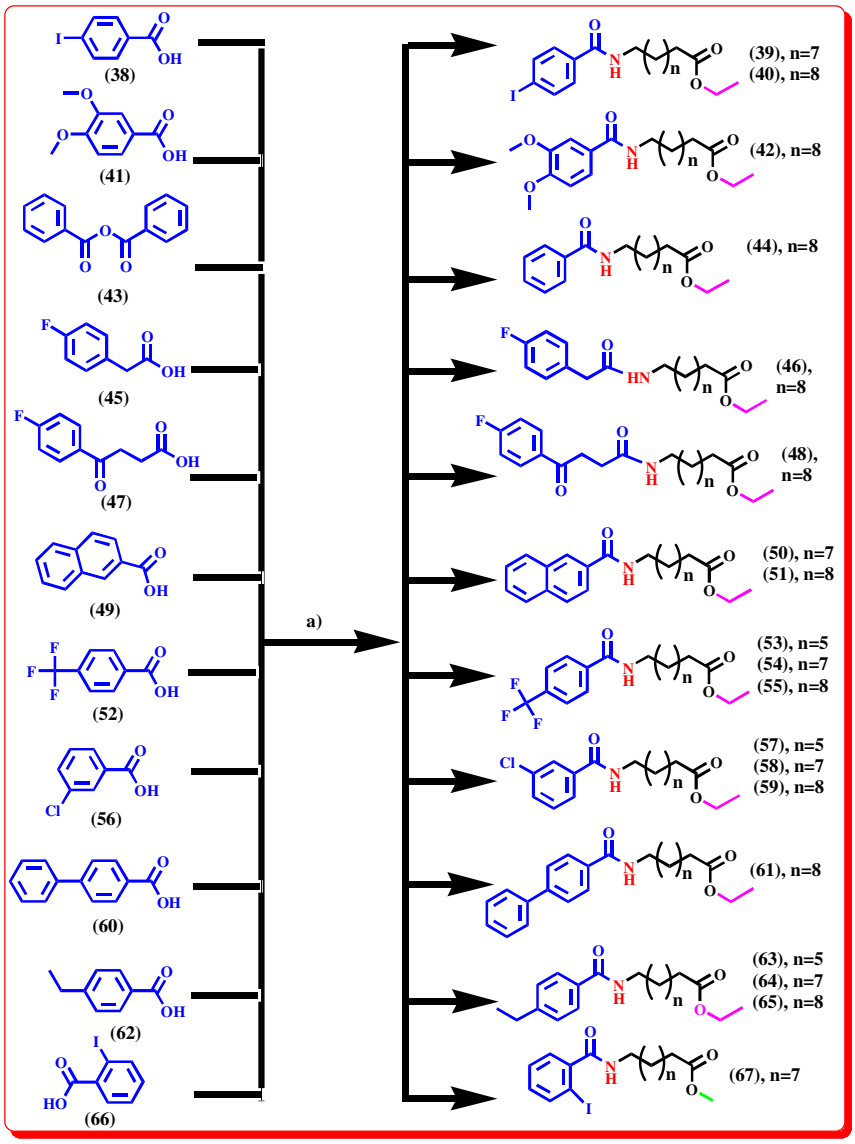

Scheme-2.4: Synthesis of the aromatic amide-myristate derivatives.

Reagents and conditions: (a) 5ml DMF, 1.1 TEA, 1.1 DCC, stirring over night at room temperature, TLC ($CHCl_3$), evaporation, extraction ethyl acetate /H_2O, purification by column chromatography $CHCl_3$: Hexane (40:60; v/v).

The aromatic amidated-alkanoic acid ethyl ester [11-benzoylaminoundecanoic acid ethyl ester **(44)**, 8-(4-trifluoromethyl-benzoylamino)-octanoic acid ethyl ester **(53)**, 8-(4-ethyl-benzoylamino)-octanoic acid ethyl ester **(63)**] was then hydrolyzed under basic conditions to give the acid form [11-benzoylaminoundecanoic acid **(68)**, 8-(4-trifluoromethyl-benzoylamino)-octanoic acid **(69)**, 8-(4-ethyl-benzoylamino)-octanoic acid **(70)**] respectively. In addition **(68)** was coupled to n-propylamine using standard peptide chemistry affording the amide analogue [n-(10-propylcarbamoyldecyl)-benzamide **(71).**

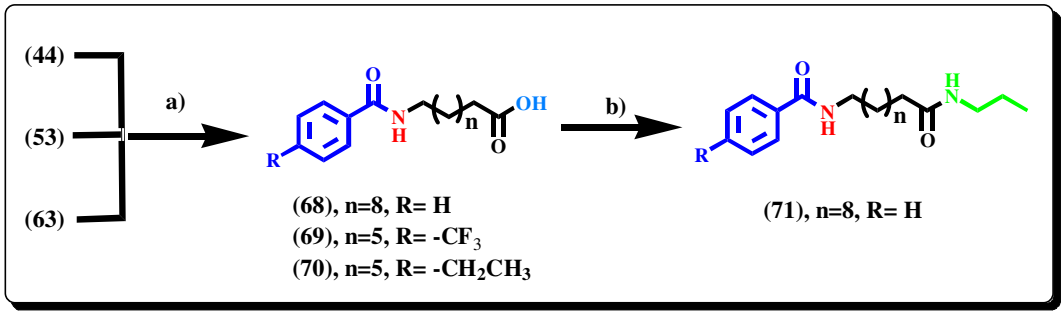

Scheme-2.5: Synthesis of (**68,69,70,71).**

Reagents and conditions: (a) NaOH 5% H_2O:EtOH 1:2, heating at 50ºC for 30minutes, TLC 100% $CHCl_3$, acidification with HCl, evaporation to dryness, extraction with ethylacetate; (b) 5ml DMF, 1.1eq DCC, 1eq NHS, Stirring overnight at room temperature, TLC 100% $CHCl_3$, 1.1eq propylamine, evaporation, extraction, purification by column chromatography [$CHCl_3$: Hexane (40:60; v/v)], recrystallization from ethanol, filtration.

2.2 Biological evaluation:

2.2.1 *In vitro* Assessment of Cellular Auto-phosphorylation Activity in Ba/F3 BCR-ABL cells:

We utilized Ba/F3, murine B lymphocytes cells, transfected with BCR-ABL gene for the evaluation of the cellular auto-phosphorylation activity of the different compounds. We noticed that responsiveness to allosteric inhibitors such as GNF-2 is a cell-type specific and also depends on the size of BCR-ABL. As shown in figure-2.3 while activity of Imatinib was comparable against p185 and p210 BCR-ABL, activity of GNF-2 was varied. GNF-2 was less effective in inhibiting cellular auto-phosphorylation of Ba/F3 with p210 BCR-ABL compared to p185 BCR-ABL. We screened our compounds for inhibitory activity of the p210 BCR-ABL

auto-phosphorylation function. Compounds were evaluated in duplicate in three concentrations 200µM, 100µM and 50µM. BCR-ABL transfected cells were treated for one hour and viability of the cells were determined using Trypan blue exclusion assay and the lysates were used to evaluate cellular auto-phosphorylation.

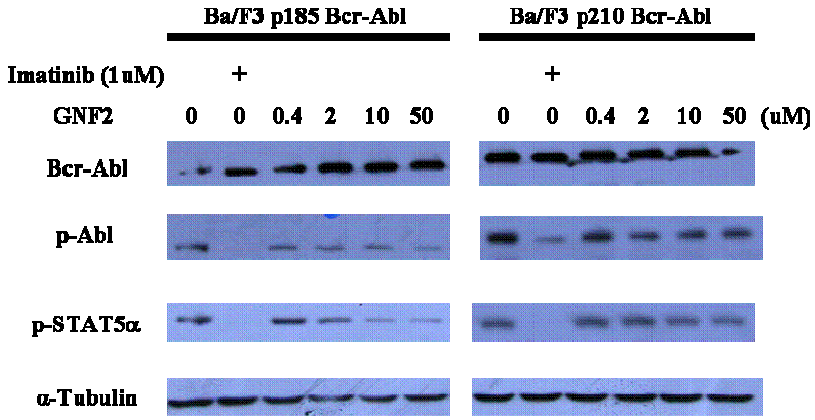

Figure-2.3: Auto-phosphorylation inhibition of STAT5α and p185, p210 BCR-ABL by GNF-2.

2.2.2 Toxicity and inhibition of BCR-ABL cellular auto-phosphorylation by MAJY compounds

The following compounds (Table 2.1) were synthesized and their biological activities were carried out for inhibition of BCR-ABL cellular auto-phosphorylation.

Table-2.1-a: Codes and structures of the synthesized compounds

Compound	Compound code	Structure	Compound	Compound code	Structure
20,21	MAJY 1	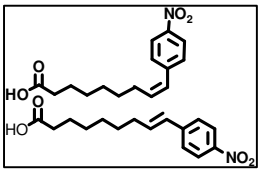	**18,19**	MAJY 3	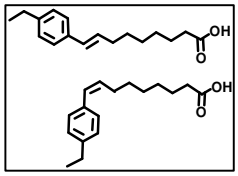
14,15	MAJY 2	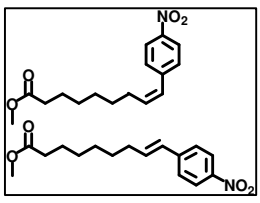	**12,13**	MAJY 4	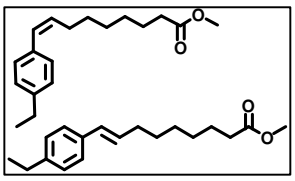

Table-2.1-b: Codes and structures of the synthesized compounds

Compound	Compound code	Structure	Compound	Compound code	Structure
22,23	MAJY 11	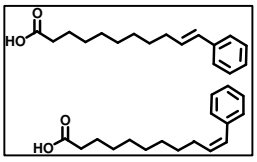	**53**	MAJY 39	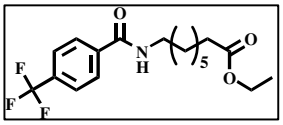
16,17	MAJY 12	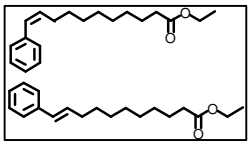	**70**	MAJY 40	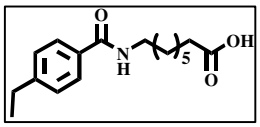
25	MAJY 16	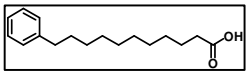	**63**	MAJY 41	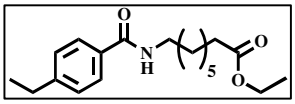
28	MAJY 23	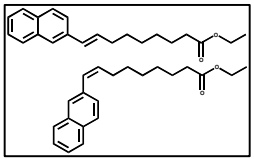	**68**	MAJY 42	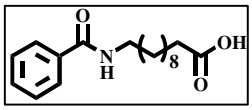
16	MAJY 24	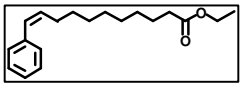	**44**	MAJY 43	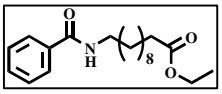
24	MAJY 25	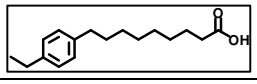	**57**	MAJY 45	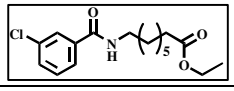
26, 27	MAJY 26	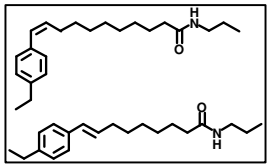	**58**	MAJY 54	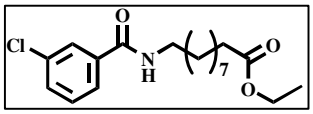
22	MAJY 27	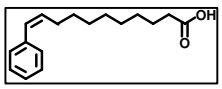	**54**	MAJY 55	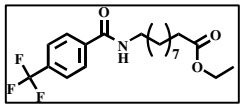
29	MAJY 28	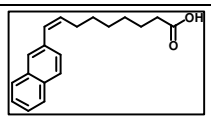	**50**	MAJY 56	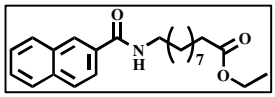
30	MAJY 31	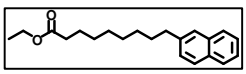	**64**	MAJY 61	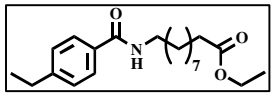
69	MAJY 38	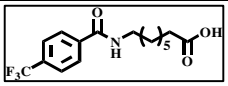	**39**	MAJY 63	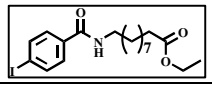

Table-2.1-c: Codes and structures of the synthesized compounds

Compound	Compound code	Structure	Compound	Compound code	Structure
67	MAJY 65	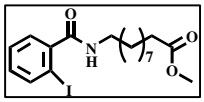	**65**	MAJY 72	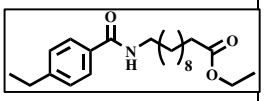
61	MAJY 67	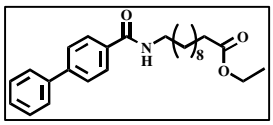	**71**	MAJY 73	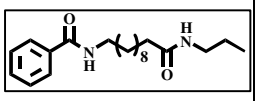
51	MAJY 68	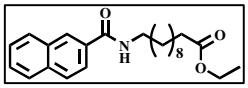	**46**	MAJY 74	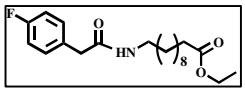
42	MAJY 69	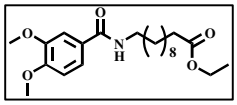	**48**	MAJY 75	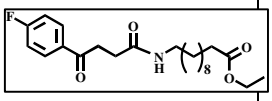
59	MAJY 70	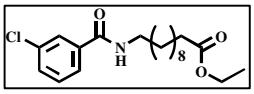	**55**	MAJY 76	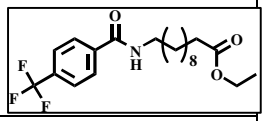
40	MAJY 71	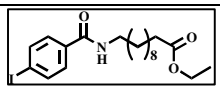			

The inhibition of BCR-ABL auto-phosphorelation of our compounds at 100 µM was shown in (figure 2.4-A, B and C) with comparison to 1 µM Imatinib and 10 µM GNF-2. The cellular viability of the treated cells was also followed. The criteria for selections were activity in cellular auto-phosphorylation assay with minimal observed cytotoxicity. .

A

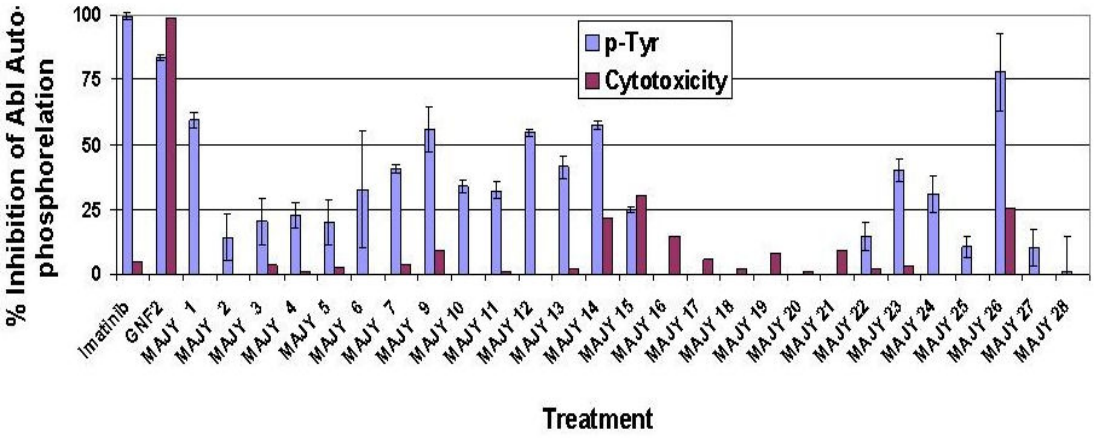

Figure-2.4-A: Toxicity and inhibition of BCR-ABL cellular auto-phosphorylation by MAJY compounds. Percentage of BCR-ABL auto-phosphorylation (blue) and viability inhibition (red).

B

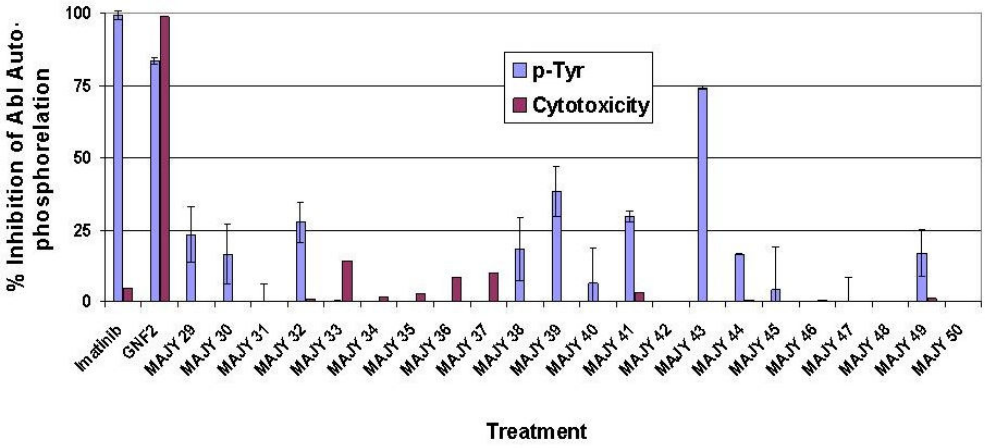

Figure-2.4-B: Toxicity and inhibition of BCR-ABL cellular auto-phosphorylation by MAJY compounds. Percentage of BCR-ABL auto-phosphorylation (blue) and viability inhibition (red).

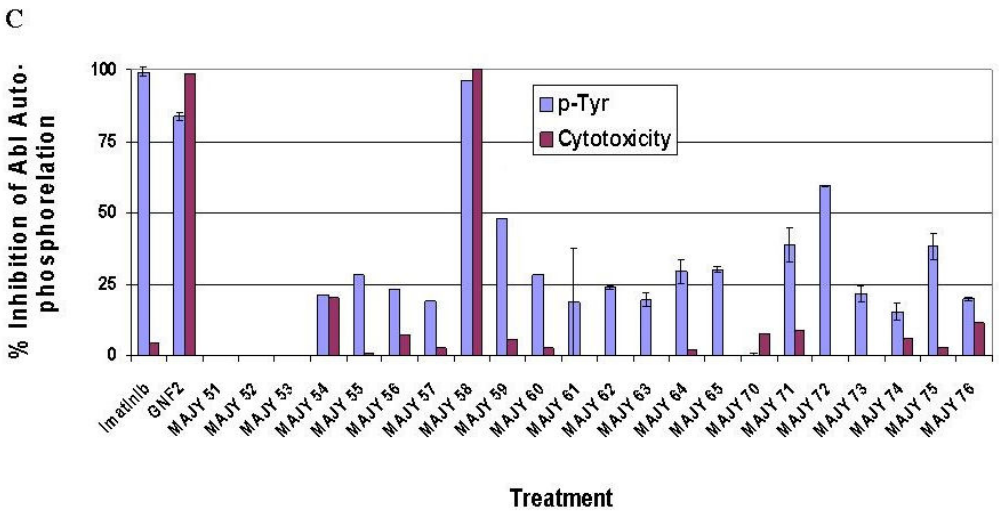

Figure-2.4-C: Toxicity and inhibition of BCR-ABL cellular auto-phosphorylation by MAJY compounds. Percentage of BCR-ABL auto-phosphorylation (blue) and viability inhibition (red).

2.2.3 Toxicity and inhibition of T315I mutated BCR-ABL cellular auto-phosphorylation by MAJY compounds

Compounds that exhibited good activities in the Ba/F3 BCR-ABL cell lines were tested for their ability to affect auto-phosphorylation of T315I mutated BCR-ABL form. The results are shown in figure-2.5 which demonstrates that the most active compound in inhibiting auto-phosphorylation of mutated T315I BCR-ABL was MAJY-43. However, presence of MAJY-43 showed no noticeable toxicity.

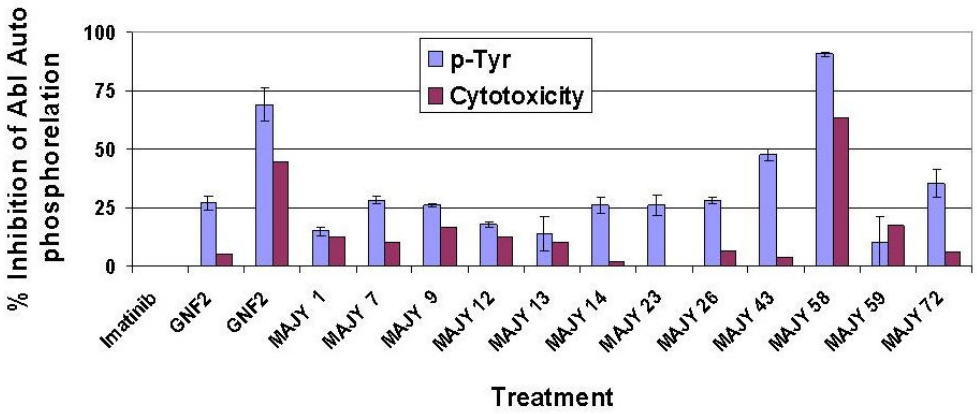

Figure-2.5: Toxicity and inhibition of T315I mutated BCR-ABL cellular auto-phosphorylation by MAJY compounds. Percentage of BCR-ABL auto-phosphorylation (blue) and viability inhibition (red).

MAJY-43 was tested for its ability to affect levels of phosphorylated native, E255K and T315I mutated BCR-ABL by immune blotting (Figure-2.6).

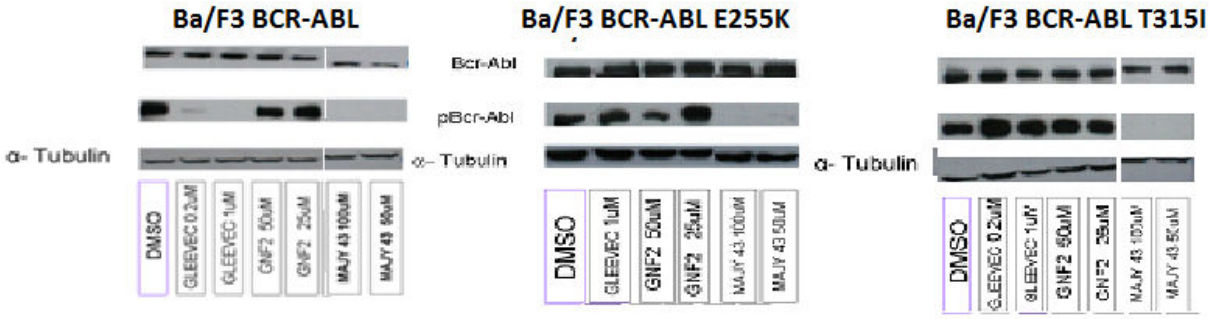

Figure-2.6: Inhibition of phosphorylated native, E255K and T315I mutated BCR-ABL by MAJY-43 in compare to GNF-2 and Imatinib.

Imatinib at 1µM was active in inhibiting BCR-ABL auto-phosphorylation in Ba/F3 cells carrying native BCR-ABL, but failed to do so in cells carrying the T315I and E255K mutate BCR-ABL. In contrast, GNF-2 at 25 µM and 50 µM was not effective in inhibiting BCR-ABL auto-phosphorylation in all cells tested. Treatment of Ba/F3 cells containing BCR-ABL with MAJY-58 caused the complete elimination of BCR-ABL apparently by degradation mechanism. MAJY-58 exhibited a dose-dependent effect and exerted its effect in all Ba/F3 cells tested. In contrast, MAJY-43 treatment inhibits BCR-ABL auto-phosphorylation without lowering the levels of BCR-ABL itself. In addition, MAJY-43 exhibited a dose dependent effect and it was active in inhibiting auto-phosphorylation of Ba/F3 cells carrying native, T315I and E255K mutated forms of BCR-ABL.

2.2.4 Colonigenicity inhibition:

Anchorage-independent growth of cells is a typical characteristic of the tumorigenicity of cancer cells *in vitro*. Different of our compounds were tested for their ability to affect colonogenicity of Ba/F3 harboring native and T315I BCR-ABL constructs. Figure-2.7 shows that Imatinib at 1 µM was active in inhibiting colonogenicity of Ba/F3 cells carrying native BCR-ABL, but not T315I mutated BCR-ABL. Higher Imatinib concentration (10 µM) was active in inhibiting colonogenicity of both cell lines. GNF-2 at higher concentration (50 µM)

also was active in inhibiting Ba/F3 cells carrying native and T315I mutated BCR-ABL. Our compounds showed variable potency in inhibiting Ba/F3 cells carrying BCR-ABL constructs. Interestingly, most compounds showed comparable activity against colonogenicity of Ba/F3 harboring native or T315I BCR-ABL constructs (Figure-2.7: A and B).

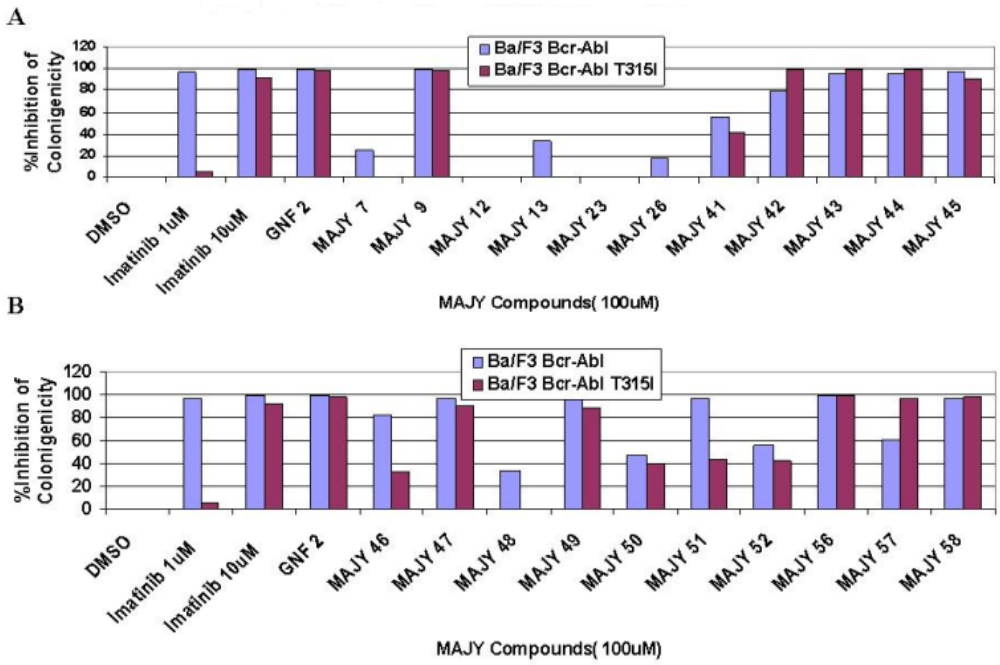

Figure-2.7-A,B: Colonigenicity Inhibition of Ba/F3 cells carrying the native and T315I mutated BCR-ABL constructs by MAJY compounds.

C.

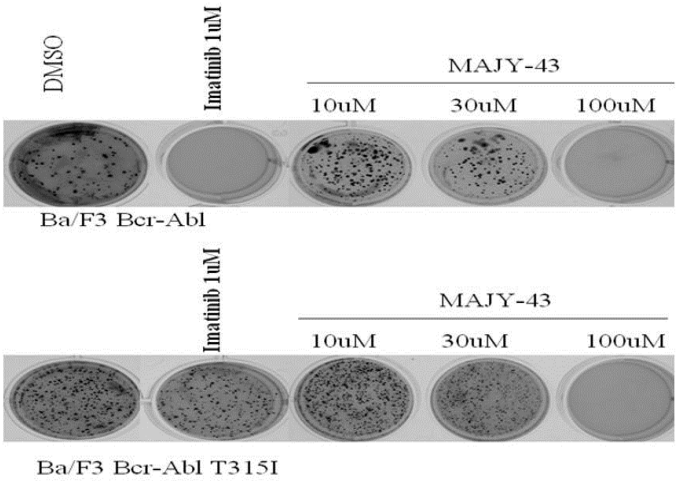

	IC_{50} in Ba/F3 Bcr-Abl	IC_{50} in Ba/F3 Bcr-Abl T315I
MAJY-43	13uM ±1.414	28uM ± 1.606

Figure-2.7-C: Colonigenicity Inhibition of Ba/F3 cells carrying the native and T315I mutated BCR-ABL constructs by MAJY 43 at (10, 30, 100 µM) in comparison to 1µM Imatinib.

Results presented in Figure-2.7A and 2.7C demonstrated that MAJY-43 was active in inhibiting colonogenicity of both Ba/F3 BCR-ABL and Ba/F3 BCR-ABL T315I with IC_{50} of 13 and 28 µM, respectively.

2.3 BCR-ABL Structure-Activity Relationships (SAR) of aromatic myristates:

Cell-based structure-activity relationship is used to guide the optimization and diversification of ligands that are capable of binding to the MBP. Set of different aromatic myristate analogues has been synthesized and evaluated for their potency to inhibit the auto-phosphorylation in Ba/F3 BCR-ABL transfected cells carrying either the native or the T315I mutated form in comparison to Imatinib and GNF-2.

2.3.1 Effect of Aromatic and Aromatic-ene Myristates:

A series of aromatic myristate analogues were predicted to bind the MBP in higher affinity, but actually the biological results showed that some of these compounds were inactive as much as their intermediates due to their structure feature such as 11-phenylundecanoic acid MAJY-16 **(25)** and its intermediate 11-phenylundec-10-enoic ethyl ester (MAJY-12) **(17)**.

Three major compounds (MAJY-12, -24 and -26), among the phenyl- myristate analogues, showed good activity against the inhibition of BCR-ABL auto-phosphorylation. Knowing that, the presence of (MAJY-26) **(26,27)** caused slightly cytotoxicity to the treated cells. MAJY-26 comprises *p*-ethylphenyl ring conjugated to double bond on one end and n-propylamide on the other.

The myristate mimic (MAJY-16) **(25)** demonstrated no inhibition activity as a result of replacing the three methylenes residing at the ω-terminal with aromatic ring, while keeping identical distance between the two terminals of the resulting fatty acid. However, when a double bond was conjugated to the aromatic ring (MAJY-12) **(17)** an improved activity was observed. While, when the double bond was shifted to two methylenes from the aromatic ring (MAJY-4) **(12,13)** the activity drops.

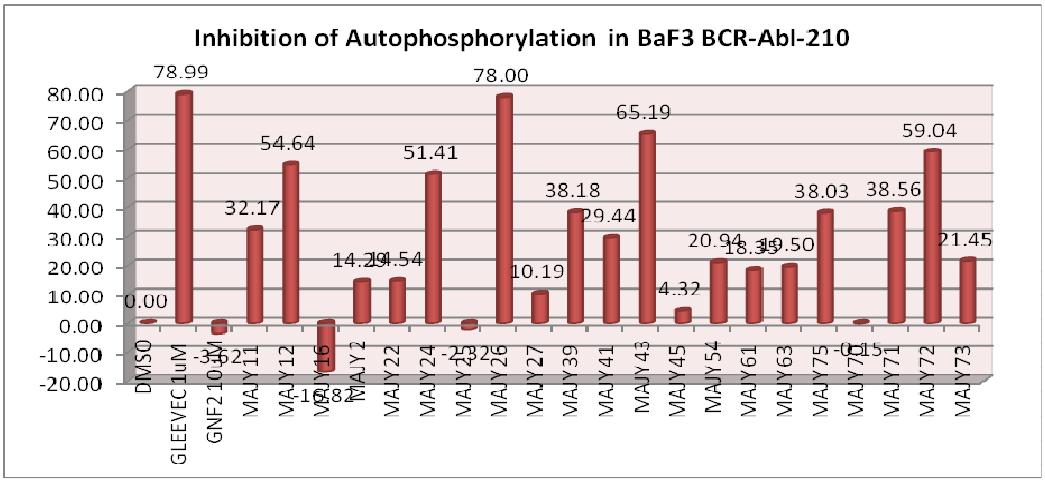

Figure-2.8: Inhibitory effect of aromatic myristate analogues on inhibiting auto-phosphorylation of Ba/F3 p210 BCR-ABL.

11-phenylundec-10-enoic ethyl ester (MAJY-12) **(17)** exhibits a partial effect on inhibiting auto-phosphorylation of Ba/F3 p210 BCR-ABL [54% vs. at 100 µM], which is not seen in the presence of 11-phenylundecanoic acid (MAJY-16) **(25**) derivatives, this indicates that the aromatic moiety at the ω-terminal of the alkanoic acid is not sufficient by itself to improve the activity of the myristate, however, when the aromatic moiety was conjugated to the olefin there was improvement in the activity, indicating that additional lipophilic interaction with the MBP is a contributor to improved activity. When the aromatic moiety was shifted two methylenes toward the amidated carboxy terminal (MAJY-26), the activity at 100 µM was improved by 50% and was comparable to Imatinib at 1 µM. Worth to note that at these conditions both (MAJY-12, -24 and -26) were much more efficient in inhibiting the auto-phosphorylation of BCR-ABL than the newly reported allosteric inhibitor GNF-2 at 10 µM. Whereas GNF-2 showed more effect on inhibiting auto-phosphorylation of T315I mutated BCR-ABL form than (MAJY-12 and -26) do.

Moreover, we thought that increasing the hydrophobicity of MAJY's compounds by using the naphthyl derivatives conjugated to the double bond (MAJY-23 and -28) would increase the hydrophobic interactions in the binding to MBP. But indeed, no activity was shown as expected against the auto-phosphorylation of Ba/F3 p210 BCR-ABL.

2.3.2 Effect of substitution and chain length of the aromatic-amide myristates:

After the identification of MAJY-12 **(17)** and -26 **(26,27)** as two lead compounds with partial inhibitory effect of BCR-ABL expressing Ba/F3 cells, set of MAJY-12 **(17)** analogues were prepared but with replacement of the alkene moiety with amide group and keeping the overall structural features including the distance between the aromatic moiety and the carboxyl. We thought that the insertion the amide group to MAJY-12 **(17)** would be capable of participating in hydrogen bond system, which would enhance the affinity of predicted analogues with the (MBP).[MAJY-12 **(17)** ➔ MAJY-43 **(44)**].

Several aromatic- amide myristates analogues with different substituent on the aromatic ring were synthesized and evaluated on their activity to inhibit BCR-ABL auto-phosphorylation in

Ba/F3 cells. MAJY-43 was the most active compound among all the synthesized compounds in this work; MAJY-43 **(44)** was comparable to that of MAJY-12 **(17).** We thought by keeping the chain length between the carboxy and the aromatic ring constant similar to MAJY-43 with changing the substituent this might improve the activity. This includes 4-iodobenzoyl MAJY-71 **(40)**, 3,4-dimethoxybenzoyl- MAJY-69 **(42),** 4-fluorophenylacetyl- MAJY-74 **(46)**, 4-(4-Fluoro-phenyl)-4-oxobutyryl- MAJY-75 (**48),** 1-naphthoyl- MAJY-68 **(51)**, 4-Trifluoromethylbenzoyl- MAJY-76 **(55),** 3-chlorobenzoyl MAJY-70 **(59)**, 4-biphenylcarbonyl- MAJY-67 **(61)** and 4-ethylbenzoyl- MAJY-72 **(65)**. The second trial was shortening the chain length by one methylene [MAJY-63 **(39)**, -56 **(50)**, -55 **(54)**, -54 **(58)**, -61 **(64)**, and -65 **(67)**]. In another trial the chain length was shortened by three methylenes [MAJY-39 **(53)**, -45 **(57)** and -41 **(63)**]. None of these compounds showed the inhibitory potency that [MAJY-12 **(17)**, -26 **(26)**, or -43 **(44)**] did. The only derivative endowed with comparable potency was MAJY-72 **(65)**, in which the aromatic ring is adjacent to the amide with an ethyl group at *para* position with a chain length of ten methylenes separating the amide terminus. The three compounds MAJY-12 **(17)**, -43 **(44)** or -72 **(65)** have the same length of the methylene chain between the carboxy terminal to the aromatic ring that is ten, while in MAJY-26 **(26)** there are eight methylenes. Besides, all active compounds have a double bond or amide group adjacent to aromatic moiety.

We expected that increasing the lipophilicity by using large aromatic entities compounds MAJY-67 **(61)** and -68 **(51)** would increase the activity more than MAJY-43 does, but unfortunately such compounds were devoid of activity, this might indicate about the tightness of the MBP. On the other hand, activity drops when the aromatic ring was 4-iodinated **(40)**, 3-chlorinated **(59)**, or when trifluoromethyl resides at *p*-position at the phenyl **(55)**. In addition, shifting the aromatic moiety by single methylene e.g. MAJY-74 **(46)** or four atoms e.g. MAJY-75 **(48)** also did not enhance the activity.

2.3.3 Effect of Carboxyl Terminal Modification on inhibiting the BCR-ABL auto-phosphorylation activity:

Some modifications were carried out at the carboxyl terminal of MAJY-12 and -43 (ester, acid

and amide) and were also assessed to see its effect on inhibiting the BCR-ABL auto-phosphorylation activity. While keeping the chain length between the carboxyl terminal and the aromatic ring in MAJY-43 **(44)**, the ester carboxyl terminal was hydrolyzed and them amidated to afford MAJY-42 **(68)** and MAJY-73 **(71)** respectively. MAJY-43 **(44)** was the most active compound in inhibiting the auto-phosphorylation of Ba/F3 p210 BCR-ABL, while its acid form MAJY-42 **(68)** didn't show any inhibitory effect and the amidated carboxy terminal MAJY-73 **(71)** had about 18% inhibitory effect underlying the role of the amide functional group as compared to the acid form (Figure-2.4 B and C).

The activity of inhibiting the BCR-ABL auto-phosphorylation is affected by modifying the carboxy terminal (ester, carboxylate, amide) MAJY-4, -3, and -26 respectively as shown in Figure-2.9. While keeping the length between the carboxyl terminal and the ω-methyl, the aromatic ring was displaced by two methylenes toward the carboxyl terminal to give rise to the ester form MAJY-4 **(12,13)** and the acid form MAJY-3 **(18,19)**. Both compounds exert decreased auto-phosphorylation inhibitory effect when compared to GNF-2 or Imatinib. Whereas, the ester form MAJY-26 **(26,27)** - that has 4-ethyphenyl moiety conjugated to a double bond at the ω-terminal and n-propyl amide at the carboxy terminal- was obtained with improved inhibitory activity.

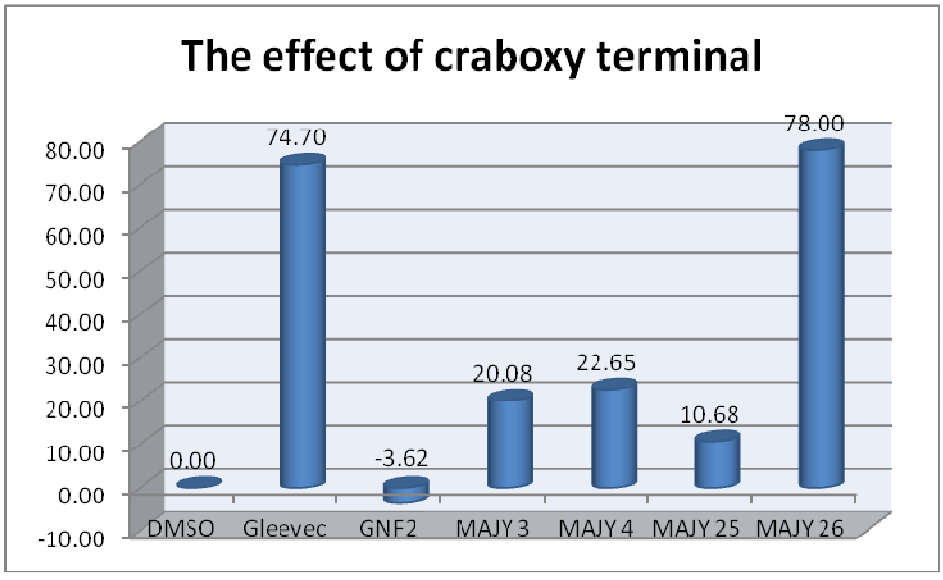

Figure-2.9: The effect of the modifying the carboxy terminal (ester, carboxylate, amide) on the activity Gleevec: 1 µM, GNF-2: 50 µM, MAJYs (3, 4, 25, 26: 100 µM for 1 hr).

Compared to MAJY-26 **(26,27)** which inhibited 78% of the activity BCR-ABL auto-phosphorylation, however, MAJY-4 **(12,13)** had 20% inhibitory effect underlying the role of the amide functional group as compared to the ester. Both acid forms **(18)** and **(19)** were less effective than the ester **(12,13)** and the amide **(26,27)**. Nonetheless, all myristate analogues (MAJYs at 100 μM) were more effective in inhibiting the auto-phosphorylation of BCR-ABL-210 (WT) in BaF3 than did GNF-2 (50 μM).

In the case of MAJY-3 (**18,19**) and its analogues the ester exerts comparable activity to the free carboxylate derivative MAJY-4 **(12,13)**; however the activity drops to half when the double bond was reduced in case of free carboxylate analogue MAJY-25 **(24)**. When the carbonyl terminal was amidated with n-propylamine in MAJY-26 **(26)** an approximate fourfold increase in the activity was observed. Indicating that the combination of an aromatic ring conjugate to a double bond positioned six methylenes from a terminal amide has a potentiating effect on the auto-phosphorylation inhibition.

Chapter Three: Conclusion

3. Conclusion

This research constitutes a new potential approach to the treatment of CML and could become complementary to the current method of cure by ATP competitors (Imatinib, Dasatinib, Nilotinib, and others). The BCR-ABL inhibitor Imatinib is now the first-choice treatment for all newly diagnosed CML patients, but the initial striking efficacy of this drug has been overshadowed by the development of clinical resistance. Resistance is mostly caused by the acquisition of point mutations in BCR/ABL. The "gatekeeper" mutation T315I confers resistance against all available molecular therapy approaches.

Allosteric inhibition represents a promising new strategy for the design of kinase inhibitors with improved selectivity and utility in overcoming drug resistance. On chemical biology, this research produces new molecular entities that could be useful for studying several biomolecular systems in which myristoyl binding pocket exist.

We have presented sets of candidate derivatives of myristate that could provide effective inhibitors of BCR-ABL by targeting the myristate binding pocket (MBP) in the BCR-ABL oncoprotein. We have shown the ability of different myristate analogues at 100 µM to inhibit the auto-phosphorylation in Ba/F3 BCR-ABL transfected cells carrying either the native or the T315I mutated form in comparison to 1 µM Imatinib and 10 µM GNF-2. Four major novel compounds (**MAJY-12, -26, -43** and **-72)** displayed improved inhibitory potency against the auto-phosphorylation of BCR-ABL. The most potent compound was discovered is **MAJY-43 (44)**, which exhibited a dose dependent effect and it was active in inhibiting auto-phosphorylation of Ba/F3 cells carrying native, T315I and E255K mutated forms of BCR-ABL.

We thought that replacing the double bond which increases the lipophilicity in **MAJY-12 (17)** by the amide group **MAJY-43 (44)** - while keeping the distance between the aromatic moiety and the carboxyl terminal constant – is capable of participating in hydrogen bond system, might enhanced the affinity with the (MBP). Whereas using different substituent on the phenyl ring didn't improve the inhibitory potency against the auto-phosphorylation of BCR-ABL in

comparison to **MAJY-43 (44)**. The chain length between the aromatic moieties to the carboxyl terminal didn't show that much effect in the inhibitory activity of some compounds. On the other hand, the carboxyl terminal has high effect in inhibiting the auto-phosphorylation of Ba/F3 p210 BCR-ABL in the case of **MAJY-26, -43** and their derivatives. **MAJY-43** was also active in inhibiting colonogenicity of both Ba/F3 BCR-ABL and Ba/F3 BCR-ABL T315I with IC_{50} of 13 and 28 μM, respectively.

In summary, the *in vitro* data strongly suggest that a variety of promising lead compounds have been identified and found to bind potently to the MBP and inhibit BCR-ABL activity.

Chapter Four: Experimental Part

4.1. Materials:

Chemicals: triphenylphosphine (PPh_3), n-butyl lithium (1.6M) (n-BuLi), benzaldehyde, naphthalene-2-carbaldehyde, 11-bromoundecanoic acid, 10-bromodecanoic acid, 8-bromooctanoic acid, 4-iodobenzoic acid, benzoic anhydride, propyl amine, 3,4-dimethoxybenzoic acid, (4-fluorophenyl)-acetic acid, 4-(4-fluorophenyl)-4-oxobutanoic acid, 1-naphthoic acid, 4-trifluoromethylbenzoic acid, 3-chlorobenzoic acid, biphenyl-4-carboxylic acid, 4-ethylbenzoic acid, N-carbethoxy phthalimide, 2-iodobenzoic acid, 6-methoxybenzofuran-2-carboxylic acid, acetic anhydride, 4-aminobenzoic acid, tetrachlorophthalic anhydride, dicyclohexylcarbodiimide (DCC), N-hydroxysuucinimide (NHS), sodium sulfate (Na_2SO_4), dimethylformamimde (DMF), dichloromethane (DCM), ethyl acetate (Eth. Ac.), triethylamine (TEA), methanol (MeOH), ethanol (EtOH), hexane, chloroform ($CHCl_3$) and pyridine were purchased from ACROS Chemicals Ltd. Potassium iodide (KI), ammonium hydroxide (NH_4OH 25%), sodium hydroxide (NaOH), tetrahydrofuran (THF), dioxane and sulfuric acid (H_2SO_4) were purchased from Aldrich Chemicals Ltd. and were used without further purification. Silica gel (Silica gel 60 (0.040-0.063 mm)), thin layer chromatography (TLC Silica gel 60 F_{254}) sheets were all purchased from Merck Ltd.

Deuterated solvents: D_2O, $CDCl_3$ (Chloroform-d), DMSO-d_6 (Deuterated dimethyl sulfoxide (d_6)) was purchased from ACROS Chemicals Ltd.

^{1}H-NMR and ^{13}C-NMR:

Data were collected using Varian Unity Inova 500 MHz spectrometer equipped with a 5-mm switchable and data were processed using the VNMR software.

4.2. Synthesis and characterization of group (I) myristate analogues:

4.2.1. Synthesis of 11-phenylundec-10-enoic acid ethyl ester (MAJY-12) (16,17):

Step (A): 10-bromodecanoic acid ethyl ester (5).

10-bromodecanoic **(2)** (5g, 39.8mmol) were dissolved in ethanol 12ml (398mmol) and 25 ml

of toluene and 10 drops of H_2SO_4 was added to the mixture which was then refluxed using Dean Stark apparatus for 3 hrs until all of the acid has been converted to ester (TLC: MeOH/ $CHCl_3$ (1:99; v/v)). The solvent was then removed and the product was dissolved in ethyl acetate and extracted against water. Organic layer was dried to give 5g of 10-bromodecanoic acid ethyl ester **(5)**.

TLC [MeOH:$CHCl_3$ 1:99; v/v)], R_f (I_2) = 7.1/8.5= 0.83

Product: colorless oil

Yield: 5g (90%).

^{1}H-NMR 300 MHz ($CDCl_3$) δ(ppm) 1.3 (m, 10H), 1.35 (t, 3H), 1.6 (m, 2H), 1.8 (m, 2H), 2.27 (t, 2H), 3.37 (t, 2H), 4.1 (q, 2H).

Step (B): 10-triphenylphosphoniumethyldecanoate bromide salt (8).

10-bromodecanoic acid ethyl ester **(5)** (4g, 14.3mmol) and (3.75g, 14.3mmol) of triphenylphosphine were refluxed in 25 ml dioxane for 10 days. Reaction was followed by TLC ($CHCl_3$). Dioxane was evaporated to dryness and then the salt was washed with diethyl ether 20 ml three times. The oily layer was separated and dried under vacuum to give 7g of 10-triphenylphosphoniumethyldecanoate bromide salt **(8)**.

TLC ($CHCl_3$) R_f= 1.5/8.5= 0.18

Product: brownish oil (gummy).

Yield: 7g (90%).

^{1}H-NMR 300 MHz ($CDCl_3$) δ(ppm) 1.27 (m, 19H), 1.65 (m, 2H), 2.2 (t, 2H), 4.1 (q, 2H), 7.65-7.8 (m, 15H).

Step (C): 11-phenylundec-10-enoic acid ethyl ester (16,17).

(8) (1.5g, 2.77mmol) was dissolved in 20ml dry THF. The solution was cooled to -78 ˚C. Under N_2 atmosphere, n-BuLi (1.6M in hexane; 2.1ml, 3.3mmol) were added drop wisely while the temperature was kept at -78 ˚C. When the addition of n-BuLi was completed the reaction was stirred at -78 ˚C for 40 minutes. At this stage, benzaldehyde (0.28ml, 2.77mmol) was added drop wisely and reaction was stirred for additional hour under inert atmosphere at -78 ˚C. The reaction mixture was allowed to elevate to room temperature and the stirring continued for overnight. Reaction progress was mentored using TLC $CHCl_3$: hexane (40:60;

v/v). When the reaction was over, it was quenched by adding 10% aqueous hydrochloric acid. The reaction mixture was partitioned between DCM and distilled water. The organic fractions were pooled and dried over anhydrous Na_2SO_4. After filtering off the solids desired product was purified using column chromatography [$CHCl_3$: hexane (20:80; v/v)] to give 278mg of pure 11-phenylundec-10-enoic acid ethyl ester **(16,17)**,

TLC ($CHCl_3$: hexane (40:60; v/v) R_f= 6.3 /8.5= 0.74

Product: off-white oil.

Yield: 0.28g (37.5%).

^{1}H-NMR 300 MHz ($CDCl_3$) δ(ppm) 1.27(m, 8H), 1.30 (t, 3H), 1.4-1.45 (m, 2H), 1.55 (m, 2H), 2.18-2.2 (dt, 2H), 2.34(t, 2H), 4.1 (q, 2H), 5.65(dt, 1H), 6.4 (d, 1H), 7.15-7.35 (m, 5H).

4.2.2. Synthesis of 11-phenylundec-10-enoic acid (22,23).

(16,17) (0.051g, 0.177mmol) was hydrolyzed by 5% NaOH : MeOH –H_2O (2:1; v/v), stirring at room temperature Reaction was followed by TLC MeOH : $CHCl_3$ (5:95; v/v). Then it was acidified by 10%HCl (dropping), extracted with three portions of DCM (25 ml/each). The organic phase was dried and weighed 35mg of pure 11-phenylundec-10-enoic acid **(22,23)**.

TLC (MeOH : $CHCl_3$ (5:95; v/v)) R_f= 2.2/7.4= 0.29

Product: white precipitate

Yield: 0.035g (76%).

^{1}H-NMR 300 MHz ($CDCl_3$) δ(ppm) 1.27(m, 8H), 1.4 (m, 2H), 1.61 (m, 2H), 2.31 (dt, 2H), 2.34 (t, 2H), 5.65(dt, 1H), 6.4(d, 1H), 7.20-7.35 (m, 5H).

4.2.3. Synthesis of 11-phenylundecanoic acid (25).

Part of 11-phenylundec-10-enoic acid **(22,23)** was reduced by H_2(g) Pd-C at100 psi for 4 hrs to obtain 11-phenyl-undecanoic acid.

4.2.4. Synthesis of 9-*p*-nitrophenyl-8-nonenoic acid (20,21)

Step 1: preparation of 8-Bromo-octanoic acid methyl ester (3)

8–Bromooctanoic acid (5g, 22.4mol) were dissolved in 15 ml methanol and 25 ml toluene and then 5 drops of H_2SO_4 was added. The mixture was refluxed using Dean Stark apparatus until

all of the acid has converted to ester (2-3 hrs) (TLC: MeOH/ $CHCl_3$ (1:99; v/v)). The solvent was then removed and the product was dissolved in ethyl acetate and extracted against water and then against 5 % $NaHCO_3$.

TLC [MeOH:$CHCl_3$ 1:99; v/v)], R_f (I_2) = 6.8/8.2= 0.83

^{1}H-NMR 300 MHz ($CDCl_3$) δ(ppm) 1.3 (m, 6H), 1.66 (m, 2H), 1.8 (m, 2H), 2.27 (t, 2H), 3.35 (t, 2H), 3.68 (s, 3H).

Step 2: 8-triphenylphosphoniumethyloctanoate bromide salt (6)

8-bromomethyloctanoate **(3)** (5g, 21.08mmol) and (5.5g, 21.08mmol) of PPh_3 in 25ml 1,4-dioxane were refluxed for 10 days. Reaction was followed by TLC ($CHCl_3$). Dioxane was evaporated to dryness and then the salt was washed with diethyl ether 20 ml three times. The oily layer was separated and dried under vacuum to give the brownish gummy 8-triphenylphosphoniumethyloctanoate bromide salt **(6)**

TLC ($CHCl_3$) R_f= 1.4/8.2= 0.17

Product: brownish oil (gummy).

^{1}H-NMR 300 MHz ($CDCl_3$) δ(ppm) 1.3 (m, 10H), 1.65 (m, 2H), 2.27 (t, 2H), 3.35 (s, 3H), 7.3-7.6 (m, 15H).

Step 3: Synthesis of 9-*p*-nitrophenyl-8-nonenoic acid (20,21)

A solution of NaH (0.160g) (Sodium hydride, 60% dispersion in mineral oil) dispersed in 5ml dried DCM was added drop wisely at 0 °C to a solution of 8-triphenylphosphonium methyloctanoate bromide salt **(6)** (2.0g, 3.9 mmol) dissolving in 10 ml of dry DCM. When all of the NaH was added the mixture was warmed to room temperature and then it was refluxed for 1 hr. Then p-nitrobenzaldehyde (0.601g, 3.98mmol) dissolved in 10ml dried DCM was added drop by drop under vigorous stirring. After all the p-nitrobenzaldehyde was added the mixture was refluxed for additional 2 hours. After that EtOH and then water were added drop wisely with stirring. The solvent was then dried under vacuum and the product was dissolved in DCM and extracted against water. The DCM layer was purified by CC using [$CHCl_3$: MeOH] as eluents to afford 9-(4-nitrooxyphenyl)-non-8-enoic acid methyl ester **(*Z*-14, *E*-15)**. Then half of the product was hydrolyzed by 5% NaOH : MeOH –H_2O (2:1; v/v), stirring at room temperature Reaction was followed by TLC MeOH : $CHCl_3$ (5:95; v/v). Then it was

acidified by 10% HCl, extracted with three portions of DCM (25 ml/each). The organic phase was dried to give 9-(4-nitrooxyphenyl)-non-8-enoic acid **(20, 21)**.

^{1}H-NMR 300 MHz ($CDCl_3$) δ(ppm) 1.3 (m,4H), 1.32-1.35 (m,2H), 1.6 (m,2H), 2.0 (dt,2H), 2.23 (t,2H), 6.3 (dt,1H), 6.6 (d,1H), 7.61 (d,2H), 8.22 (d,2H).

4.2.5. Synthesis of (9-(4-ethylphenyl)-non-8-enoic acid (18,19)

A solution of NaH (0.093g) (Sodium hydride, 60% dispersion in mineral oil) dispersed in 5ml dried DCM was added drop wisely at 0 °C to a solution of 8-triphenylphosphonium methyloctanoate bromide salt (1.17 g, 2.28 mmol) dissolved in 10 ml of dry DCM. When all of the NaH was added the mixture was warmed to room temperature and then was refluxed for 3 hrs. Then p-ethylbenzaldehyde (0.30 ml, 2.17 mmol) dissolved in 10ml dried DCM was added drop wisely under vigorous stirring. After all the *p*-ethylbenzaldehyde was added the mixture was refluxed for additional 2 hours. After that EtOH and then water were added drop wisely with stirring. The solvent was then dried under vacuum and the product was dissolved in DCM and extracted against water. The DCM layer was purified by CC using [$CHCl_3$: MeOH] as eluents to afford (9-(4-ethylphenyl)-non-8-enoic acid methyl ester **(*Z*-12, *E*-13)**. Half of the product was hydrolyzed by 5% NaOH : MeOH –H_2O (2:1; v/v), stirring at room temperature Reaction was followed by TLC MeOH : $CHCl_3$ (5:95; v/v). Then it was acidified by 10% HCl, extracted with three portions of DCM (25 ml/each). The organic phase was dried to (9-(4-ethylphenyl)-non-8-enoic acid **(18,19).**

TLC (MeOH : $CHCl_3$ (5:95; v/v)) R_f= 2.0/6.8= 0.29

Product: off-white precipitate

^{1}H-NMR 300 MHz ($CDCl_3$) δ(ppm) 1.24 (t,3H), 1.3-1.35 (m,6H), 1.6 (m,2H), 2.0 (dt,2H), 2.24 (t,2H), 2.6 (t,2H), 5.58 (dt,1H), 6.4 (d,1H), 7.10 (d,2H), 7.27 (d,2H).

4.3. Synthesis of naphthyl-myristate analogues (subgroup C).

4.3.1. Synthesis of 9-naphthalen-2-yl-non-8-enoic acid ethyl ester (28)

Step 1: synthesis of 8-bromooctanoic acid ethyl ester (4).

8-Bromooctanoic **(1)** (5g, 22.4mmol) were dissolved in ethanol 12ml (398mmol) and 25 ml of

toluene and 10 drops of H_2SO_4 was added to the mixture which was then refluxed using Dean Stark apparatus for 3 hrs until all of the acid has been converted to ester (TLC: MeOH/ $CHCl_3$ (1:99; v/v)). The solvent was then removed and the product was dissolved in ethyl acetate and extracted against water. Organic layer was dried to give of 8-bromooctanoic acid ethyl ester **(4)**.

TLC [MeOH:$CHCl_3$ 1:99; v/v)], R_f (I_2) = 7.0/8.3= 0.84

Product: colorless oil

^{1}H-NMR 300 MHz ($CDCl_3$) δ(ppm) 1.29 (m, 6H), 1.35 (t, 3H), 1.65 (m, 2H), 1.8 (m, 2H), 2.27 (t, 2H), 3.35 (t, 2H), 4.1 (q, 2H).

Step (B): 8-triphenylphosphoniumethyloctanoate bromide salt (7).

8-Bromooctanoic acid ethyl ester **(5)** (4g, 15.9mmol) and (6.9g, 15.9mmol) of triphenylphosphine were refluxed in 25 ml dioxane for 10 days. Reaction was followed by TLC ($CHCl_3$). Dioxane was evaporated to dryness and then the salt was washed with diethyl ether 20ml three times. The oily layer was separated and dried under vacuum to give 8-triphenylphosphoniumethyloctanoate bromide salt **(7)**.

TLC ($CHCl_3$) R_f= 1.5/8.5= 0.18

Product: brownish oil (gummy).

^{1}H-NMR 300 MHz ($CDCl_3$) δ(ppm) 1.25-1.3 (m, 12H), 1.65 (m, 2H), 2.25 (t, 2H), 4.1 (q, 2H), 7.3-7.6 (m, 15H).

Step (C): Synthesis of 9-naphthalen-2-yl-non-8-enoic acid ethyl ester (28)

7-Ethoxycarbonyl-heptyl)-triphenyl-phosphonium; bromide **(7)** (4.76g, 9.26 mmol) was dissolved in 20ml dry THF. The solution was cooled to -78 ˚C. Under N_2 atmosphere, n-BuLi (1.6M in hexane; 7ml, 11.1 mmol) were added drop wisely while the temperature was kept -78 ˚C. When the addition of n-BuLi was completed the reaction was stirred at -78 ˚C for 1 hour. At this stage, 2-naphthaldehyde (1.45g. 9.26 mmol) was added drop wisely and reaction was stirred for additional hour under inert atmosphere and -78 ˚C. The reaction mixture was allowed to elevate to room temperature and the stirring continued for overnight. Reaction progress was mentored using TLC $CHCl_3$: hexane (40:60; v/v). When the reaction was over, it was quenched by adding 10% aqueous hydrochloric acid. The reaction mixture was

partitioned between DCM and distilled water. The organic fractions were pooled and dried over anhydrous Na_2SO_4. After filtering off the solids desired product was purified using column chromatography [$CHCl_3$: hexane (20:80; v/v)] to give 0.47 g of pure 9-naphthalen-2-yl-non-8-enoic acid ethyl ester (28),

TLC ($CHCl_3$: hexane (20:80; v/v) R_f= 6.3 /8.5= 0.74

Product: white precipitate

Yield: 0.047g (1.6%).

^{1}H-NMR 300 MHz ($CDCl_3$) δ(ppm) 1.25-1.29 (m, 4H), 1.3 (t,3H), 1.35 (m, 2H), 1.68 (m, 2H), 2.2 (dt, 2H), 2.3 (t, 2H), 4.1 (q, 2H), 5.80 (dt, 1H), 6.41 (d, 1H), 7.44-7.72 (m, 7H).

4.3.2. Synthesis of 9-Naphthalen-2-yl-non-8-enoic acid (29)

(28) (0.047g, 0.15mmol) was hydrolyzed by 5% NaOH : MeOH –H_2O (2:1; v/v), stirring at room temperature Reaction was followed by TLC MeOH : $CHCl_3$ (5:95; v/v). Then it was acidified by 10%HCl (dropping), extracted with three portions of DCM (25 ml/each). The organic phase was dried and weighed 25.8mg of 9-naphthalen-2-yl-non-8-enoic acid **(29)**.

TLC (MeOH : $CHCl_3$ (5:95; v/v)) R_f= 2.8/7.4= 0.38

Product: white precipitate

Yield: 0.026g (65%).

^{1}H-NMR 300 MHz ($CDCl_3$) δ(ppm) 1.25-1.29 (m, 4H), 1.35 (m, 2H), 1.68 (m, 2H), 2.2 (dt, 2H), 2.27 (t, 2H), 5.90 (dt, 1H), 6.41 (d, 1H), 7.44-7.72 (m, 7H).

4.3.3. Synthesis of 9-Naphthalen-2-yl-nonanoic acid ethyl ester (30)

Part of 9-naphthalen-2-yl-non-8-enoic acid ethyl ester **(28)** was reduced by H_2(g) Pd-C at100 psi for 4 hrs to obtain 9-naphthalen-2-yl-nonanoic acid ethyl ester **(30).**

4.4 Synthesis of group (II) myristate analogues

4.4.1. Synthesis of aminoalkanoic acid ethyl esters [8-aminooctanoic acid ethyl ester (35), 10-aminodecanoic acid ethyl ester (36), 11-aminoundecanoic acid ethyl ester (37)].

General Procedure.

Bromoalkanoic acid (4.00mmol) [8-bromooctanoic acid (**1**), 10-bromodecanoic acid (**2**),11-bromoundecanoic acid (**31**)] was dissolved in 5 equivalents NH_4OH 25% (3.0ml) and stirred at room temperature for 48 hours. The reaction progress was followed using TLC (MeOH:$CHCl_3$; 20:80; v/v; I_2). When the reaction was over as indicated by the disappearance of the starting material the volatiles were evaporated to dryness under reduced pressure. The precipitate was dissolved in (15ml) EtOH neat and heated to reflux for 1 hour. The mixture was allowed to cool to ambient temperature and precipitates were filtered off. The precipitate was washed with additional 10 ml ethanol and filtrates were collected and evaporated to dryness to give a white precipitate of corresponding aminoalkanoic acid [8-aminooctanoic acid **(32),** 10-aminodecanoic acid **(33)**, 11-aminoundecanoic acid **(34)**,]. The amino acid **[(32), (33), (34)]** was then dissolved in 25ml EtOH and cooled in ice-bath, gaseous hydrochloric acid HCl was bubbled until the pH turned to strongly acidic (pH=1). The ice bath was removed and the mixture was heated reflux. The esterification was followed using TLC (MeOH: $CHCl_3$; 20:80; v/v; I_2). When affirming the total conversion of the amino acid to ester form the reaction mixture was cooled to room temperature and the volatiles evaporated under reduced pressure to dryness. The off-white precipitate of corresponding aminoalkanoic acid ethyl ester [**(35)**, **(36)**, **(37)**] was collected and re-crystallized from ethanol.

11-Aminoundecanoic acid (34).

Product: White precipitate

Yield: 0.80g (100%).

^{1}H-NMR 300 MHz ($CDCl_3$) δ(ppm) 1.21 (m, 12H), 1.59 (m, 2H), 1.78 (m, 2H), 2.26 (t, 2H), 3.01 (t, 2H).

11-Aminoundecanoic acid ethyl ester (37).

Product: Off-white precipitate

Yield: 0.96g (91%).

^{1}H-NMR 300 MHz ($CDCl_3$) δ(ppm) 1.21 (m, 12H), 1.25 (t, 3H), 1.59 (m, 2H), 1.78 (m, 2H), 2.26 (t, 2H), 3.01 (t, 2H), 4.10 (q, 2H).

4.4.2. Synthesis of 11-Arylamidoundecanoic acid ethyl ester derivatives (39, 40, 42)

General Procedure:

In a 25ml round bottom flask, (0.37g, 1.5mmol) of the aromatic carboxylic acid derivative, (0.4g, 1.5mmol) [**(37)** as example], (0.34g, 1.65mmol) DCC and (0.24ml, 1.65mmol) dry triethylamine (TEA) were mixed in 5ml DMF. The reaction mixture was stirred at room temperature for the time needed for completion. The reaction progress was followed using TLC ($CHCl_3$). When the reaction was completed DMF was evaporated under reduced pressure to dryness and the mixture was portioned between the aqueous and ethyl acetate (30mlX3). The organic fractioned were pooled dried over anhydrous sodium sulfate. After filtering off the solids the volatiles were evaporated to dryness under reduced pressure. The off-white powder was purified by column chromatography using $CHCl_3$: hexane (40:60; v/v) as eluent to give the purified desired product.

11-(4-Iodobenzoylamino)-undecanoic acid ethyl ester (40).

TLC ($CHCl_3$), R_f= 2.6/8.5= 0.31

Product: white powder

Yield: 0.44g (63.8%).

^{1}H-NMR 300 MHz ($CDCl_3$) δ(ppm) 1.25-1.30 (m, 15H), 1.6 (m,2H), 1.69 (m, 2H), 2.2 (t, 2H), 3.39 (m, 2H), 4.11 (q, 2H), 6.15 (s, N-H $_{amide}$), 7.27 (d, 2H), 7.75 (d, 2H).

10-(4-Iodo-benzoylamino)-decanoic acid ethyl ester (39).

TLC ($CHCl_3$), R_f= 2.6/8.5= 0.31

Product: white precipitate

Yield: 0.43g (56.6 %).

^{1}H-NMR 300 MHz ($CDCl_3$) δ(ppm) 1.25 (m, 13H), 1.59 (m, 2H), 1.81 (m, 2H), 2.03 (t, 2H), 3.48 (m, 2H), 4.05 (q, 2H), 6.15 (s, N-H $_{amide}$), 7.25 (d, 2H), 7.74 (d, 2H).

11-(3, 4 -Dimethoxybenzoylamino)-undecanoic acid ethyl ester (42).

The crude product was purified by column chromatography $CHCl_3$ to give a white powder of **(42)**.

TLC ($CHCl_3$), R_f= 2.5/8.5= 0.29

Product: white precipitate

Yield: 0.40g (67.8%).

^{1}H-NMR 300 MHz ($CDCl_3$) δ(ppm) 1.25 (m, 15H), 1.57 (m, 2H), 1.81 (m, 2H), 2.06 (t, 2H), 3.49 (t, 2H), 3.91 (s, 6H), 4.12 (q, 2H), 6.06 (s, N-H amide), 6.85 (d, 1H), 7.12 (s, 1H), 7.18 (d, 1H).

4.4.3. Synthesis of 11-Benzoylaminoundecanoic acid ethyl ester (44).

In a 25ml round bottom flask, **(37)** (0.4g, 1.5mmol), benzoic anhydride **(43)** (0.34g, 1.5mmol) and TEA (0.25ml, 1.8mmol) were dissolved in 10ml DMF. The reaction mixture was stirring at room temperature for overnight and the completion of the reaction was indicated by TLC $CHCl_3$:Hexane (60: 40; v/v).The DMF was evaporated to dryness and crude product was extracted by $CHCl_3$ against distilled water. The organic phase was dried by Na_2SO_4 and the solvent was removed by reduced pressure. The crude product was purified by column chromatography using $CHCl_3$:Hexane (40: 60; v:v) to give 0.25g white powder of **(44)**.

TLC ($CHCl_3$), R_f= 1.5/8.6= 0.17

Product: white precipitate

Yield: 0.25g (50%).

^{1}H-NMR 300 MHz ($CDCl_3$) δ(ppm) 1.25-1.30 (m, 15H), 1.60 (m, 4H), 2.28 (t, 2H), 3.45 (t, 2H), 4.12 (q, 2H), 6.10 (s, N-H $_{amide}$), 7.48 (dd, 1H), 7.42 (m, 2H), 7.75(d, 2H).

^{13}C-NMR ($CDCl_3$, δ ppm): 15.0, 25.0, 27.25, 29.27, 29.4, 29.5, 29.52, 29.54, 29.8, 34.9, 40.05, 60.08, 76.8, 77.5, 77.8, 126.5, 128.0, 130.0, 131.0, 134.0, 135.0, 168.0, 172.0.

4.4.4. Synthesis of 11-Benzoylaminoundecanoic acid (68).

(44) (1.13g) were dissolved in 10ml of NaOH 5% (EtOH:H_2O; 2:1) and refluxed at 50 °C for 30 min. Completion of the hydrolysis was monitored by TLC ($CHCl_3$), then the reaction mixture was acidified and extracted by ethyl acetate, the organic phase was dried and the solvent was distilled off by reduced pressure to afford 1.0g of **(68)** as a white powder.

Product: white powder

Yield: 1.00g (96.6%).

^{1}H-NMR 300 MHz ($CDCl_3$) δ(ppm) 1.30 (m, 15H), 1.61 (m, 4H), 2.34 (t, 2H), 3.44 (t, 2H), 6.10 (s, N-H $_{amide}$), 7.42 (m, 3H), 7.74 (d, 2H).

4.4.5. Synthesis of N-(10-Propylcarbamoyldecyl)-benzamide (71).

In a 25ml round bottom flask, **(68)** (0.2g, 0.65mmol), NHS (0.075g, 0.65mmol) and DCC (0.15g, 0.715mmol) were dissolved in DMF (5ml as a solvent). The reaction mixture was stirring at room temperature for overnight, the completion of the reaction was indicated by TLC ($CHCl_3$). Then propyl amine (0.06ml, 0.72mmol) was added to the mixture under the same condition. DMF was evaporated to dryness; crude product was extracted by Ethyl acetate against distilled water. The organic fractions were collected and dried by Na_2SO_4. After filtering off the solids the solvent was removed under reduced pressure to one tenth of original volume. Mixture was then filtered to give a 0.137g white powder **(71)**.

TLC ($CHCl_3$), R_f= 1/8.5= 0.12

Product: white powder

Yield: 0.137g (62.3%).

^{1}H-NMR 300 MHz ($CDCl_3$) δ(ppm) 0.90 (t, 3H), 1.30 (m, 12H), 1.60 (m, 6H), 3.2 (q, 2H), 3.44 (q, 2H), 5.5 (s, N-H $_{amide}$), 6.23 (s, N-H $_{amide}$), 7.43 (d, 3H), 7.76 (d, 2H).

4.4.6. Synthesis of 11-[2-(4-fluoro-phenyl)-acetylamino]-undecanoic acid ethyl ester (46).

In a 25ml round bottom flask, **(37)** (0.4g, 1.5mmol), (4-fluorophenyl)-acetic acid **(45)** (0.24g, 1.5mmol), DCC (0.34g, 1.65mmol) and TEA (0.23ml, 1.65mmol) were dissolved in 5ml DMF. The reaction mixture was stirring at room temperature for overnight and the completion of the reaction was indicated by TLC ($CHCl_3$). The DMF was evaporated to dryness; crude product was extracted by ethyl acetate against distilled water. The organic fractions were collected and dried by Na_2SO_4. After filtering off the solids the solvent was removed under reduced pressure. The crude product was purified by column chromatography using $CHCl_3$: Hexane (40: 60; v/v) to give 75mg of **(46)** as a white powder.

TLC ($CHCl_3$), R_f= 1.7/8.5= 0.2

Product: yellowish precipitate

Yield: 0.15g (27.8%).

^{1}H-NMR 300 MHz ($CDCl_3$) δ(ppm) 1.25-1.30 (m, 15H), 1.6 (m, 4H), 2.26 (t, 2H), 3.19 (m, 2H), 3.51 (s, 2H), 4.10 (q, 2H), 5.36 (s, N-H $_{amide}$), 7.02 (d, 2H), 7.21 (d, 2H).

4.4.7. Synthesis of 11-[4-(4-Fluorophenyl)-4-oxobutyrylamino]-undecanoic acid ethyl

ester (48).

In a 25ml round bottom flask, **(37)** (0.4g, 1.5mmol), 4-(4-fluorophenyl)-4-oxobutanoic acid **(47)** (0.29g, 1.5mmol), DCC (0.25g, 1.65mmol) and TEA (0.23ml, 1.65mmol) were dissolved in 5ml DMF. The reaction mixture was stirring at room temperature for overnight and the completion of the reaction was indicated by TLC ($CHCl_3$). Then DMF was evaporated to dryness, product was extracted by ethyl acetate against distilled water, the organic phase was dried by Na_2SO_4 and the solvent was removed by reduced pressure to afford a mixture as a yellowish solution. The crude product was purified by column chromatography using $CHCl_3$: Hexane (40:60 v/v) to give 0.32g yellowish powder of **(48)**.

TLC ($CHCl_3$), R_f= 1.7/8.5= 0.2

Product: yellowish powder

Yield: 0.32g (40%).

^{1}H-NMR 300 MHz ($CDCl_3$) δ(ppm) 1.27(m, 15H), 1.79(m, 2H), 1.98(m, 2H), 2.79(t, 2H), 3.38(t, 4H), 3.71(m, 2H), 4.1(q, 2H), 7.15(d, 2H), 8.03(d, 2H).

4.4.8. Synthesis of 11-[(Naphthalene-2-carbonyl)-amino]-undecanoic acid ethyl ester (51).

In a 25ml round bottom flask, **(37)** (0.40g, 1.5mmol), 1-naphthoic acid **(49)** (0.28g, 1.65mmol), DCC (0.34g, 1.65mmol) and TEA (0.23ml, 1.65mmol) were dissolved in 5ml DMF. The reaction mixture was stirring at room temperature for overnight and the completion of the reaction was indicated by TLC ($CHCl_3$). Then DMF was evaporated to dryness, product was extracted by ethyl acetate against distilled water, the organic phase was dried by Na_2SO_4 and the solvent was removed by reduced pressure to afford a mixture as an off-white powder. The crude product was purified by column chromatography using 100% $CHCl_3$ to give a white powder of **(51)**.

TLC ($CHCl_3$), R_f= 6/8.7= 0.69

Product: white powder

Yield: 0.52g (90%).

^{1}H-NMR 300 MHz ($CDCl_3$) δ(ppm) 1.25 (m, 15H), 1.57 (m, 2H), 1.83 (m, 2H), 2.16 (t, 2H), 3.48 (t, 2H), 3.88 (q, 2H), 7.15 (s, N-H $_{amide}$), 7.43-7.50 (d, 2H), 7.57 (d, 2H), 7.88 (d, 2H), 7.91 (s, 1H).

4.4.9. Synthesis of 10-[(Naphthalene-2-carbonyl)-amino]-decanoic acid ethyl ester (50).

In a 25ml round bottom flask, **(36)** (0.40g, 1.59mmol), **(49)** (0.27g, 1.59mmol), DCC (0.36g, 1.75mmol) and TEA (0.24ml, 1.75mmol) were dissolved in 5ml DMF. The reaction mixture was stirring at room temperature for overnight and the completion of the reaction was indicated by TLC ($CHCl_3$). Then DMF was evaporated to dryness, product was extracted by ethyl acetate against distilled water, the organic phase was dried by Na_2SO_4 and the solvent was removed by reduced pressure to afford a mixture as an off-white powder. The crude product was purified by column chromatography using 100% $CHCl_3$ to give 0.45g white powder of **(50)**.

TLC ($CHCl_3$), R_f= 4.2/9= 0.47

Product: white powder

Yield: 0.45g (76%).

^{1}H-NMR 300 MHz ($CDCl_3$) δ(ppm) 1.25 (m, 13H), 1.50 (m, 2H), 1.73 (m, 2H), 2.13 (t, 2H), 3.43 (t, 2H), 3.86 (q, 2H), 7.00 (s, N-H $_{amide}$), 7.23 (dd, 2H), 7.42 (d, 2H), 7.52 (d, 2H), 7.87 (s, 1H).

4.4.10. Synthesis of 11-(4-Trifluoromethylbenzoylamino)-undecanoic acid ethyl ester (55).

In a 25ml round bottom flask, **(37)** (0.40g, 1.5mmol), 4-trifluoromethyl-benzoic acid **(52)** (0.28g, 1.5mmol), DCC (0.34g, 1.65mmol) and TEA (0.23ml, 1.65mmol) were dissolved in 5ml DMF. The reaction mixture was stirring at room temperature for overnight and the completion of the reaction was indicated by TLC ($CHCl_3$). Then DMF was evaporated to dryness, product was extracted byethyl acetate against distilled water the organic phase was dried by Na_2SO_4 and the solvent was removed by reduced pressure to afford a mixture as an off-white powder. The crude product was purified by column chromatography using 100% $CHCl_3$ to give **(55)** as a white precipitate.

TLC ($CHCl_3$), R_f= 2.7/8.8= 0.31

Product: white precipitate

Yield: 0.095g (24%).

^{1}H-NMR 300 MHz ($CDCl_3$) δ(ppm) 1.25-1.30 (m, 15H), 1.57 (m, 2H), 1.80 (m, 2H), 2.00 (t, 2H), 3.48 (m, 2H), 4.1 (q, 2H), 6.08 (s, N-H $_{amide}$), 7.66 (d, 4H).

4.4.11. Synthesis of 10-(4-Trifluoromethylbenzoylamino)-decanoic acid ethyl ester (54).

In a 25ml round bottom flask, **(36)** (0.40g, 1.59mmol), **(52)** (0.30g, 1.59mmol), DCC (0.36g, 1.75mmol) and TEA (0.24ml, 1.75mmol) were dissolved in 5ml DMF. The reaction mixture was stirring at room temperature for overnight and the completion of the reaction was indicated by TLC ($CHCl_3$). Then DMF was evaporated to dryness, product was extracted by Ethyl acetate against distilled water, the organic phase was dried by Na_2SO_4 and the solvent was removed by reduced pressure to afford a mixture as an off-white powder. The crude product was purified by column chromatography using 100% $CHCl_3$ to give 0.33g **(54)** as a white powder.

TLC ($CHCl_3$), R_f= 2.7/8.8= 0.31

Product: white precipitate

Yield: 0.33g (53.8%).

^{1}H-NMR 300 MHz ($CDCl_3$) δ(ppm) 1.25-1.30 (m, 13H), 1.49 (m, 2H), 1.76 (m, 2H), 2.00 (t, 2H), 3.44 (m, 2H), 4.1 (q, 2H), 6.08 (s, N-H $_{amide}$), 7.20 (d, 2H), 7.61 (d, 2H).

4.4.12. Synthesis of 8-(4-Trifluoromethyl-benzoylamino)-octanoic acid ethyl ester (53).

In a 25 ml one-necked flask were charged, the residue of 8-aminooctanoic acid ethyl ester (**35**) (0.5 g, 2.23 mmol), α,α,α-triflouro-P-toluic acid (**52**) (0.423g, 2.23mmol), DCC (0.475g, 2.23mmol) TEA (0.306ml, 2.25mmol) and ethyl acetate (5ml as solvent). The reaction mixture was stirring at room temperature for 36hours, the completion of the reaction was indicated by TLC (100% $CHCl_3$), the mixture was filtered, and the solvent was distilled off by reduced pressure, the residue was purified by column chromatography 100% $CHCl_3$.

TLC ($CHCl_3$), R_f= 2.3/8.2= 0.28

Product: white precipitate

Yield: 0.40g (50%).

NMR results : 1H-NMR (300 MHz, CDCl3): $\delta_{(ppm)}$ 1.2 (t, 3H), 1.6 (m, 8H), 1.7(m, 4H), 2.3 (t, 2H), 2.7 (t, 2H), 3.5(q, 2H), 4.1 (q, 2H), 6.2 (brd, N-H $_{amide}$), 7.7 (d, 2H), 7.9 (d, 2H).

4.4.13. Synthesis of 8-(4-Trifluoromethyl-benzoylamino)-octanoic acid (69)

In a 25ml round bottom flask, **(53)** (0.05 g, 46mmol) were dissolved in 10ml of NaOH 5%

(EtOH:H_2O; 2:1) and refluxed at 50 °C for 30 min. Completion of the hydrolysis was monitored by TLC ($CHCl_3$), then the reaction mixture was acidified and extracted by ethyl acetate, the organic phase was dried and the solvent was distilled off by reduced pressure to afford **(69)** as an off- white powder.

NMR results: 1H-NMR (300 MHz, CDCl3): $\delta_{(ppm)}$, 1.6 (m, 8H), 1.7(m, 4H), 2.3 (t, 2H), 2.3 (t, 2H), 3.5(q, 2H), 6.2 (brd, N-H $_{amide}$), 7.7 (d, 2H), 7.9 (d, 2H).

4.4.14. Synthesis of 11-(3-Chlorobenzoylamino)-undecanoic acid ethyl ester (59).

In a 25ml round bottom flask, **(37)** (0.40g, 1.5mmol), 3-chlorobenzoic acid **(56)** (0.32g, 1.65mmol), DCC (0.34g, 1.65mmol) and TEA (0.23ml, 1.65mmol) were dissolved in 5ml DMF. The reaction mixture was stirring at room temperature for overnight and the completion of the reaction was indicated by TLC ($CHCl_3$). Then DMF was evaporated to dryness, product was extracted by ethyl acetate against distilled water, the organic phase was dried by Na_2SO_4 and the solvent was removed by reduced pressure to afford a mixture as an off-white powder. The crude product was purified by column chromatography using 100% $CHCl_3$ to give **(59)** with some impurities of DCU which was then re-crystallized by ethyl acetate to afford 0.20g of **(59)** as a white powder.

TLC ($CHCl_3$), R_F= 1.7/8.8= 0.19

Product: white powder

Yield: 0.20 g (36%).

^{1}H-NMR 300 MHz ($CDCl_3$) δ(ppm) 1.25 (m, 15H), 1.59 (m, 2H), 1.83 (m, 2H), 2.02 (t, 2H), 3.50 (t, 2H), 4.07 (q, 2H), 6.03 (s, N-H $_{amide}$), 7.35 (dd, 1H), 7.42 (d, 2H), 7.53 (s, 1H).

4.4.15. Synthesis of 10-(3-Chlorobenzoylamino)-decanoic acid ethyl ester (58).

In a 25ml round bottom flask, **(36)** (0.40g, 1.59mmol), **(56)** (0.25g, 1.59mmol), DCC (0.36g, 1.75mmol) and TEA (0.24ml, 1.75mmol) were dissolved in 5ml DMF. The reaction mixture was stirring at room temperature for overnight and the completion of the reaction was indicated by TLC ($CHCl_3$). Then DMF was evaporated to dryness, product was extracted by ethyl acetate against distilled water, the organic phase was dried by Na_2SO_4 and the solvent was removed by reduced pressure to afford a mixture as an off-white powder. The crude product was purified by column chromatography using 100% $CHCl_3$ to give **(58)** 0.39g as a

white powder.

TLC ($CHCl_3$), R_f= 1.7/8.8= 0.19

Product: white powder

Yield: 0.39g (69.3%).

^{1}H-NMR 300 MHz ($CDCl_3$) δ (ppm) 1.25 (m, 13H), 1.59 (m, 2H), 1.83 (m, 2H), 2.02 (t, 2H), 3.50 (t, 2H), 4.07 (q, 2H), 6.03 (s, N-H $_{amide}$), 7.35 (dd, 1H), 7.42 (d, 2H), 7.53 (s, 1H).

4.4.16. Synthesis of 8-(3-Chlorobenzoylamino)-octanoic acid ethyl ester (57).

In a 25ml round bottom flask, 8-aminooctanoic acid ethyl ester **(35)** (0.40g, 1.7mmol), **(56)** (0.28g, 1.7mmol), DCC (0.38g, 1.87mmol) and TEA (0.26ml, 1.87mmol) were dissolved in 5ml DMF. The reaction mixture was stirring at room temperature for overnight and the completion of the reaction was indicated by TLC ($CHCl_3$). Then DMF was evaporated to dryness, product was extracted by ethyl acetate against distilled water, the organic phase was dried by Na_2SO_4 and the solvent was removed by reduced pressure to afford a mixture as an off-white powder. The crude product was purified by column chromatography using 100% $CHCl_3$ to give 0.42g **(57)**.

TLC ($CHCl_3$), R_f= 2.1/8.8= 0.24

Product: white powder

Yield: 0.34g (57.9%).

^{1}H-NMR 300 MHz ($CDCl_3$) δ(ppm) 1.20 (m, 9H), 1.60 (m, 2H), 1.82 (m, 2H), 2.02 (t, 2H), 3.50 (t, 2H), 4.09 (q, 2H), 6.05 (s, N-H $_{amide}$), 7.35 (dd, 1H), 7.42 (d, 2H), 7.53 (s, 1H).

4.4.17. Synthesis of 11-[(Biphenyl-4-carbonyl)-amino]-undecanoic acid ethyl ester (61).

In a 25ml round bottom flask, **(37)** (0.40g, 1.5mmol), biphenyl-4-carboxylic acid **(60)** (0.22g, 1.5mmol), DCC (0.34g, 1.65mmol) and TEA (0.23ml, 1.65mmol) were dissolved in 5ml DMF. The reaction mixture was stirring at room temperature for overnight and the completion of the reaction was indicated by TLC ($CHCl_3$). Then DMF was evaporated to dryness, product was extracted by ethyl acetate against distilled water, the organic phase was dried by Na_2SO_4 and the solvent was removed by reduced pressure to afford a mixture as an off-white powder. The crude product was purified by column chromatography using 100% $CHCl_3$ to give **(61)** as a white powder.

TLC ($CHCl_3$), R_f= 2.8/9= 0.31

Product: white powder

Yield: 0.6g (96.8%).

^{1}H-NMR 300 MHz ($CDCl_3$) δ(ppm) 1.21-1.30 (m, 15H), 1.55 (m, 2H), 1.82 (m, 2H), 2.05 (t, 2H), 3.52 (m, 2H), 4.13 (q, 2H), 6.16 (s, N-H $_{amide}$), 7.44 (d, 3H), 7.62 (d, 4H).

4.4.18. Synthesis of 11-(4-Ethylbenzoylamino)-undecanoic acid ethyl ester (65).

In a 25ml round bottom flask, **(37)** (0.40g, 1.5mmol), 4-ethyl-benzoic acid **(62)** (0.22g, 1.5mmol), DCC (0.34g, 1.65mmol) and TEA (0.24ml, 1.65mmol) were dissolved in 5ml DMF. The reaction mixture was stirring at room temperature for overnight and the completion of the reaction was indicated by TLC ($CHCl_3$). Then DMF was evaporated to dryness, product was extracted by ethyl acetate against distilled water, the organic phase was dried by Na_2SO_4 and the solvent was removed by reduced pressure to afford a mixture as an off-white powder. The crude product was purified by column chromatography using 100% $CHCl_3$ to give 0.33g white powder of **(65)**.

TLC ($CHCl_3$), R_f= 2.5/8.7= 0.29

Product: white powder

Yield: 0.33g (61.8%).

^{1}H-NMR 300 MHz ($CDCl_3$) δ(ppm) 0.85 (t, 3H), 1.21-1.30 (m, 15H), 1.52 (m, 2H), 1.78 (m, 2H), 2.28 (t, 2H), 2.66 (q, 2H), 3.47 (t, 2H), 4.11 (q, 2H), 6.06 (s, N-H $_{amide}$), 7.23 (d, 2H), 7.44 (d, 2H).

4.4.19. Synthesis of 10-(4-Ethylbenzoylamino)-decanoic acid ethyl ester (64).

In a 25ml round bottom flask, **(36)** (0.40g, 1.58mmol), **(62)** (0.24g, 1.58mmol), DCC (0.36g, 1.7mmol) and TEA (0.24ml, 1.7mmol) were dissolved in 5ml DMF. The reaction mixture was stirring at room temperature for overnight and the completion of the reaction was indicated by TLC (100% $CHCl_3$). Then DMF was evaporated to dryness, product was extracted by ethyl acetate against distilled water, the organic phase was dried by Na_2SO_4 and the solvent was removed by reduced pressure to afford a mixture as an off-white powder. The crude product was purified by column chromatography using 100% $CHCl_3$ to give 0.25g of **(64).**

TLC ($CHCl_3$), R_f= 2.5/8.7= 0.29

Product: white powder

Yield: 0.25g (44.6%).

^{1}H-NMR 300 MHz ($CDCl_3$) δ(ppm) 0.85 (t, 3H), 1.26 (m, 13H), 1.58 (m, 2H), 1.80 (m, 2H), 2.12 (t, 2H), 2.65 (q, 2H), 3.46 (t, 2H), 4.12 (q, 2H), 6.06 (s, N-H $_{amide}$), 7.24 (d, 2H), 7.45 (d, 2H).

4.4.20. Synthesis of 8-(4-Ethyl-benzoylamino)-octanoic acid ethyl ester. (63)

In a 25 ml one-necked round bottom flask **(35)** (0.5 g, 2.23 mmol), **(62)** (0.335g, 2.23mmol), DCC (0.475g, 2.23mmol) and TEA (0.306ml, 2.25mmol) were dissolved in 5ml DMF The reaction mixture was stirring at room temperature for 36hr, The completion of the reaction was indicated by TLC (100% $CHCl_3$), the mixture was filtered, and the solvent was distilled-off by reduced pressure, the residue was purified by column chromatography (100% $CHCl_3$).

TLC ($CHCl_3$), R_f= 2.1/8.2= 0.26

Product: white powder

NMR results : 1H-NMR (300 MHz, CDCl3): $\delta_{(ppm)}$ 1.3 (m, 6H), 1.6 (m, 6H), 1.8(m, 4H), 2.2 (t, 2H), 2.7 (q, 2H), 3.5(q, 2H), 4.05 (q, 2H), 6.2 (brd, N-H $_{amide}$), 7.2 (d, 2H), 7.5 (d, 2H).

4.4.21. Synthesis of 8-(4-Ethyl-benzoylamino)-octanoic acid (70)

In a 25ml round bottom flask, **(63)** (0.05g, 46mmol) were dissolved in 10ml of NaOH 5% (EtOH:H_2O; 2:1) and refluxed at 50 °C for 30 min. Completion of the hydrolysis was monitored by TLC ($CHCl_3$), then the reaction mixture was acidified and extracted by ethyl acetate, the organic phase was dried and the solvent was distilled off by reduced pressure to afford **(70)**.

Product: white powder

NMR results : 1H-NMR (300 MHz, CDCl3): $\delta_{(ppm)}$ 1.2 (m, 6H), 1.3 (m, 6H), 1.6(m, 4H), 2.3 (t, 2H), 2.68 (q, 2H), 3.4(q, 2H), 6.2 (brd, N-H $_{amide}$), 7.2 (d, 2H), 7.6 (d, 2H).

4.4.22. Synthesis of 10-(2-Iodo-benzoylamino)-decanoic acid ethyl ester (67).

In a 25ml round bottom flask, **(36)** (0.40g, 1.58mmol), 2-iodobenzoic acid **(66)** (0.38g, 1.58mmol), DCC (0.36g, 1.7mmol) and TEA (0.24ml, 1.7mmol) were dissolved in 5ml DMF. The reaction mixture was stirring at room temperature for overnight and the completion of the

reaction was indicated by TLC ($CHCl_3$). Then DMF was evaporated to dryness, product was extracted by $CHCl_3$ against distilled water, the organic phase was dried by Na_2SO_4 and the solvent was removed by reduced pressure to afford a mixture as an off-white powder. The crude product was purified by column chromatography using 100% $CHCl_3$ to give **(67)**.

TLC ($CHCl_3$), R_f= 3.8/8.5= 0.44

Product: white precipitate

Yield: 0.24g (34.3%).

^{1}H-NMR 300 MHz ($CDCl_3$) δ(ppm) 1.25(m, 13H), 1.58 (m, 2H), 1.80 (m, 2H), 2.1 (t, 2H), 3.50 (t, 2H), 4.12 (q, 2H), 7.08 (, 1H), 7.26 (d, 1H), 7.40 (d, 1H), 7.83 (d, 1H).

Chapter Five: References

5. References

1. Deininger M., Buchdunger E. and Druker B. J., The development of Imatinib as a therapeutic agent for chronic myeloid leukemia, Blood, 2005, 105: 2640-2653

2. Ren R., Mechanisms of BCR-ABL in the pathogenesis of chronic myelogenous leukaemia, Nature, 2005, 5(3):172-183

3. Melo J. V. and Barnes D. J., Chronic myeloid leukaemia as a model of disease evolution in human cancer, Nature, 2007, 7: 441-453.

4. Capdeville R., Buchdunger E., Zimmermann J. and Matter A., Glivec (STI571,Imatinib), A Rationally Developed, Targeted Anticancer Drug, Nature, 2002, 1:493-502

5. Druker B. J., STI571 (GleevecTM) as a paradigm for cancer therapy, Trends in Molecular Medicine, 2002, 8 (4).

6. Hantschel O., Allosteric BCR-ABL inhibitors in Philadelphia chromosome-positive acute lymphoblastic leukemia: novel opportunities for drug combinations to overcome resistance, Haematologica, 2012, 97(2) 157-159.

7. Hochhaus A., Reiter A., Skladny H., Melo JV, Sick C, Berger U, Guo JQ, Arlinghaus RB, Hehlmann R, Goldman JM and Cross NC, A novel BCR-ABL fusion gene (e6a2) in a patient with Philadelphia chromosome-negative chronic myelogenous leukemia, Blood, 1996, 88 (6): 2236-2240.

8. Salesse S and M Verfaillie C, BCR/ABL: from molecular mechanisms of leukemia induction to treatment of chronic myelogenous leukemia, Oncogene, 2002, 21: 8547 – 8559.

9. Patel D., Suthar P. M., Patel V., Singh R., BCR ABL Kinase Inhibitors for Cancer Therapy, International Journal of Pharmaceutical Sciences and Drug Research, 2010, 2(2): 80-90.

10. Patwardhan P. and D. Resh M., Myristoylation and Membrane Binding Regulate c-SRC Stability and Kinase Activity, American Society for Microbiolog (Molecular and cellular biology), 2010, 30 (17): 4094–4107

11. Ren R, The molecular mechanism of chronic myelogenous leukemia and its therapeutic implications: studies in a murine model, Oncogene, 2002, 21: 8629 – 8642,

12. Yang J., Campobasso N., Biju P M., Fisher K., Pan X., Cottom J., Galbraith S., Ho H, Zhang H., et al. Discovery and Characterization of a Cell-Permeable, Small-Molecule c-ABL Kinase Activator that Binds to the Myristoyl Binding Site, Chemistry & Biology, 2011, 18: 177–186.

13. Deininger W. N. M., Goldman M. J. and Melo V. J., The molecular biology of chronic myeloid leukemia, Blood, 2000, 96 (10): 3343-3356.
14. Cilloni D. and Saglio G., Molecular pathways: BCR-ABL, Clinical cancer research, 2012, 18 (4):930-937.
15. Hassan Quamrul A., Sharma V. S. and Warmuth M., Allosteric inhibition of BCR-ABL, Cell Cycle, 2010, 9 (18): 3710-3714.
16. Liu Y, Gray NS. Rational design of inhibitors that bind to inactive kinase conformations, Nature Chemical Biology, 2006, 2 (7):358-364.
17. Weisberg E, Manley P. W., Cowan-Jacob S. W., D. Griffin A & J, Second generation inhibitors of BCR-ABL for the treatment of imatinib resistant chronic myeloid leukemia, Nature, 2007, 7.
18. Gumireddy, K. et al. A non-ATP-competitive inhibitor of BCR-ABL overrides Imatinib resistance, The Proceedings of the National Academy of Sciences of the United States of America, 2005, 102 (6): 1992–1997.
19. O'Hare T., Walters K. D., Stoffregen P. E., Taiping J., Manley P.W., Mestan J., Cowan-Jacob S.W., Lee Y. F., Heinrich C. M., Deininger W.N. M. and Druker J. B., In vitro Activity of BCR-ABL Inhibitors AMN107 and BMS-354825 against Clinically Relevant Imatinib-Resistant ABL Kinase Domain Mutants, Cancer Research, 2005, 65 (11): 4500-4505.

20. Adrian FJ, Ding Q, Sim T, Velentza A, Sloan C, Liu Y, Zhang G, Hur W, Ding S, Manley P, et al: Allosteric inhibitors of BCR-ABL-dependent cell proliferation. Nature Chemical Biology, 2006, 2(2):95–102.
21. Nagar B., Bornmann W.G., Pellicena P., Schindler T., Veach D.R., Miller W.T., Clarkson B. and Kuriyan J., Crystal Structures of the Kinase Domain of c-ABL in Complex with the Small Molecule Inhibitors PD173955 and Imatinib (STI-571), Cancer Research, 2002, 62: 4236– 4243.
22. Hantschel O. and Superti-Furga G., Regulation of the c-Abl and Bcr-Abl Tyrosine Kinases, Nature, 2004, 5: 33-44.
23. Druker BJ., Talpaz M., Resta DJ., Peng B., Buchdunger E., Ford JM., Lydon NB., Kantarjian H., Capdeville R., et al., Efficacy and safety of a specific inhibitor of the BCR-ABL tyrosine kinase in chronic myeloid leukemia, Medicine, 2001, 344:1031–7.
24. Schindler T., Bornmann W., Pellicena P., W. Todd Miller, Clarkson B., Kuriyan J., Structural Mechanism for STI-571 Inhibition of Abelson Tyrosine Kinase, Science, 2000, 289 (5486) : 1938-1942.
25. Gorre ME, Mohammed M, Ellwood K, Hsu N, Paquette R, Rao PN, et al., Clinical resistance to STI-571 cancer therapy caused by BCR-ABL gene mutation or amplification, Science, 2001, 293:876- 80
26. Nagar B., c-ABL Tyrosine Kinase and Inhibition by the Cancer Drug Imatinib (Gleevec/STI-571), Nutrition, 2007, 137: 1518S–1523S,.
27. O'Hare T., Corbin S. A. and Druker J B., Targeted CML therapy: controlling drug resistance, seeking cure, Current Opinion in Genetics & Development, 2006, 16:92–99
28. Schiffer A. C., M.D., BCR-ABL Tyrosine Kinase Inhibitors for Chronic Myelogenous Leukemia, Medicine, 2007, 357;3.
29. Cowan-Jacob S. W.; Guez V., Fendrich G., Griffin J. D., Fabbro D., Furet P., Liebetanz J., Mestan J., Manley P. W., Imatinib (STI571) resistance in chronic myelogenous leukemia: molecular basis of the underlying mechanisms and potential strategies for treatment. Mini-reviews in Medicinal Chemistry, 2004, 4: 285–299.
30. Nardi V., Azam M., Daley GQ., Mechanisms and implications of Imatinib resistance mutations in BCR–ABL, Current Opinion in Hematology, 2004, 11 (1):35-43.

31. Hochhaus A, La Rose´e P., Imatinib therapy in chronic myelogenous leukemia: strategies to avoid and overcome resistance, Leukemia, 2004, 18:1321-1331
32. Liu Y. & Gray N. S., Rational design of inhibitors that bind to inactive kinase conformations, Nature Chemistry Biology 2006, 2: 358–364.
33. Zhang J., Yang L. P. and Gray S. N., Targeting cancer with small molecule kinase inhibitors, Nature Reviews, Cancer, 2009, 9 (31).
34. Weisberg E., Manley P. W., Breitenstein W., Bruggen J., Cowan- Jacob S. W., Ray A., et al., Characterization of AMN107, a selective inhibitor of native and mutant BCR-ABL, Cancer Cell, 2005, 7: 129–141.
35. Manley, P. W., Cowan-Jacob, S. W., Mestan, J., Advances in the structural biology, design and clinical development of BCR-ABL kinase inhibitors for the treatment of chronic myeloid leukaemia, Biochimica et biophysica acta, 2005, 1754: 3–13.
36. Vajpai, N. et al., Solution conformations and dynamics of ABL kinase-inhibitor complexes determined by NMR substantiate the different binding modes of Imatinib/Nilotinib and Dasatinib. Biological Chemistry, 2008, 283: 18292–18302.
37. Manley PW, Cowan-Jacob SW, Fendrich G, Metan J, Molecular interactions between the highly selective pan-BCR-ABL inhibitor, AMN107, and the tyrosine kinase domain of ABL, Blood, 2005, 106: (940a).
38. Weisberg E, Manley P, Mestan J, Cowan-Jacob S, Ray A and Griffin JD, AMN107 (Nilotinib): a novel and selective inhibitor of BCR-ABL, British Journal of Cancer, 2006, 94: 1765 – 1769.
39. Pluk H., Dorey K. and Superti-Furga, G., Autoinhibition of c-ABL, Cell, 2002, 108: 247–259.
40. O'Hare T and Deininger M. W., Toward a Cure For Chronic Myeloid Leukemia, Clinical Cancer Research, 2008, 14:7971-7974.
41. Wolff N. C., Veach D. R., Tong W. P., Bornmann W. G., Clarkson B. and Ilaria R L., Jr, PD166326, a novel tyrosine kinase inhibitor, has greater antileukemic activity than Imatinib mesylate in a murine model of chronic myeloid leukemia, BLOOD, 2005, 105,(10): 3995
42. Weisberg E, Geun Choi H, Ray A, Barrett R, Zhang J, Sim T, Zhou W, et al., Discovery of a small-molecule type II inhibitor of wild-type and gatekeeper mutants of

BCR-ABL, PDGFR, Kit, and SRC kinases: novel type II inhibitor of gatekeeper mutants, BLOOD, 2010, 115, 21-27.

43. Azam M., Powers J. T., Einhorn W., Huang W. S., Shakespeare W. C., et al., AP24163 Inhibits the Gatekeeper Mutant of BCR-ABL and Suppresses In vitro Resistance, Chemical biology & drug design, 2010, 75: 223–227.
44. Azam M., Seeliger M. A, Gray N. S, Kuriyan J. & Daley G. Q, Activation of tyrosine kinases by mutation of the gatekeeper threonine, Nature Structural & Molecular Biology, 2008, 15 (10).
45. Gozgit J. M., Wong M. J., Wardwell S., Tyner J. W., et al., Potent activity of ponatinib (AP24534) in models of FLT3-driven acute myeloid leukemia (AML) and other hematologic malignancies, Molecular Cancer Therapeutics, 2011, 10(6):1028-1035.
46. O'Hare T., Eide C. A., Tyner J. W., Corbin A. S., et al., SGX393 inhibits the CML mutant BCR-ABLT315I and preempts in vitro resistance when combined with nilotinib or dasatinib, The Proceedings of the National Academy of Sciences of the United States of America, 2008, 105 (14): 5507–5512
47. Denga X., Lima S. M., Zhanga J., and Gray N. S., Broad Spectrum Alkynyl Inhibitors of T315I BCR-ABL, Bioorganic and Medicinal Chemistry Letters, 2010, 20(14): 4196–4200.
48. Christopher A. Eide, Lauren T. Adrian, Jeffrey W. Tyner, et al., The ABL Switch Control Inhibitor DCC-2036 Is Active against the Chronic Myeloid Leukemia Mutant BCR-ABLT315I and Exhibits a Narrow Resistance Profile, Cancer Research, 2011, 71(9).
49. Mian A. A., Metodieva A., Badura S., Khateb M., Ruimi N., Najajreh Y., Ottmann O. G., Mahajna J. and Ruthardt M., Allosteric inhibition enhances the efficacy of ABL kinase inhibitors to target unmutated BCR-ABL and BCR-ABL-T315I, BioMed Central Cancer, 2012, 12:411
50. Nagar B, Hantschel O, A. Young M, Scheffzek K, Veach D, Bornmann W, Structural Basis for the Autoinhibition of c-ABL Tyrosine Kinase, Cell, 2003, 112: 859-871.
51. Brier S. C. S., Smithgall T. E., and Engen J. R., The ABL SH2-kinase linker naturally adopts a conformation competent for SH3 domxain binding, Protein Science, 2007, 16:572–581.

52. Hantschel O, Nagar B, Guettler S, Kretzschmar J, Dorey K, Kuriyan J and Superti-Furga G., A Myristoyl/Phosphotyrosine Switch Regulates c-ABL, Cell, 2003, 112: 845–857.
53. Deng X, Okram B, Ding Q, Zhang J, Choi Y, Adrian F J., Wojciechowski A, Zhang G, Che J, Bursulaya B, W. Cowan-Jacob S, Rummel G, Sim T, and S. Gray N, Expanding the Diversity of Allosteric BCR-ABL Inhibitors, J. Med. Chem., 2010, 53: 6934–6946.
54. Zhang J, et al., Targeting BCR-ABL by combining allosteric with ATP-binding-site inhibitors. Nature, 2010, 463:501–506.
55. Khateb M., Ruimi N., Khamisie H., Najajreh Y., Mian A., Metodieva A., Ruthardt M. and Mahajna J., Overcoming BCR-ABL T315I mutation by combination of GNF-2 and ATP competitors in an ABL-independent mechanism, BMC Cancer, 2012, 12:563.
56. Choi Y, Seeliger M. A., Panjarian S. B., Kim H., Deng X, et al., N-Myristoylated c-ABL Tyrosine Kinase Localizes to the Endoplasmic Reticulum upon Binding to an Allosteric Inhibitor, The Journal of Biological Chemistry, 2009, 284(42), 29005–29014.
57. Tanaka R., Kimura S., ABL Tyrosine Kinase Inhibitors for Overriding BCR-ABL/T315I: From the Second to Third Generation, Expert Review of Anticancer Therapy, 2008, 8(9):1387-1398.
58. Lavis L. D., The Chemistry of Abelson Tyrosine Kinase Inhibitors, Department of Chemistry, University of Wisconsin–Madison, 2006.

تطوير مركبات شبيهة بالميرستات للعمل كمثبطات لل BCR-ABL لعلاج سرطان الدم النخاعي المزمن

اعداد: نداء عودة شحادة اغريب

اشراف: د. يوسف نجاجرة

الملخص:

سرطان الدم النخاعي المزمن (CML)، هو سرطان ينشأ في نخاع العظام، ويسبب الانتشار المفرط لخلايا الدم النخاعي. العلامة الجينية لهذا المرض هو كروموسوم فيلادلفيا، الذي ينشأ بسبب تبادل جيني بين الكروموسومات 9 و 22. ونتيجة لهذا التبادل الجيني t(9;22) في كروموسوم (22) *BCR* وكروموسوم (9) *ABL* ينتج كروموسوم ملتحم جديد *BCR-ABL* الذي ينتج أنزيم التيروزين كيناز المسؤول عن تكاثر الخلايا والبقاء على قيد الحياة .غالبية مثبطات ال BCR-ABL هي مثبطات موجهة ضد موقع ارتباط جزيء الطاقة أدينوسين ثلاثي الفوسفات (ATP) المسؤول عن عملية فسفرة البروتينات. Imatinib هو أول مثبط لل-BCR-ABL منافس لجزيء ال- ATP على موقعه وقد نجح في علاج معظم حالات مرضى اللوكيميا في المراحل المبكرة من المرض. ومع ذلك، فإن بعض المرضى إما لا يستجيبوا اصلا، أو يتم تطوير مقاومة للدواء. للتغلب على هذه التحديات، تم تطوير الجيل الثاني من مثبطات ال-BCR-ABL بما في ذلك تطوير مركبات جديدة ك- Nilotinib و- Dasatinib. ومن الجدير بالذكر أن أيا من هذه الأدوية لم تكن فعالة ضد الطفرة T315I والمسماه بحارس البوابة. وهناك جهود مبذولة لتطوير مثبطات لأنزيم الكيناز تكتسب فاعليتها باليات عمل جديدة.

في هذه الأطروحة، نسلط الضوء على تطوير "مثبطات للكيناز بديلة غير تنافسية مع ال- ATP" التي تمنع نشاط انزيم الكيناز بواسطة الارتباط في موقع بعيد عن الموقع النشط للانزيم. في الوضع الطبيعي لل-ABL تنتهي سلسلة الاحماض الامينية المكونة للانزيم بحمض دهني يتكون من 14 كربونة (ميرستات)

الذي يعمل على ايقاف عملية الفسفرة لل- ABL عن طريق ادخاله في منطقة (جيب) في انزيم الكيناز مكونة من أحماض كارهة للماء يطلق عليها جيب ارتباط الميرستات (MBP). هذا الاكتشاف واضافة الى المعرفة بأن الميرستات مفقود في البروتين الناتج من ال-BCR-ABL ولكن موقع الارتباط لا زال موجودا في الانزيم حفزنا للعمل على تطوير مجموعة من المركبات الشبيهة بالميرستات للعمل كمثبطات لل -BCR ABL حيث ترتبط بشكل خاص فقط بجيب ارتباط الميرستات (MBP) في انزيم الكيناز، تم تحضير تلك المركبات وتنقيتها وتمييزها وفحص نشاطها في عملية الفسفرة وأيضا تقييم احتمالية بقاء وتكاثر الخلايا السرطانية. أظهرت نتائج الفحص المخبرية الأولية اتي اجريت على خلايا سرطانية يترجم فيها انزيم ال-BCR-ABL أهمية هذا النهج والكشف عن مشتقات للميرستات تعمل على تثبيط فسفرة ال BCR-ABL الاصلي وأيضا ال-BCR-ABL الحامل بطفرة حارس البوابة T315I . في هذا البحث تم اكتشاف مركبات جديدة (**MAJY-12**, **-26**, **-43** and **-72**) التي تعطي فاعلية تثبيط جيدة ضد فسفرة ال- BCR-ABL.